iScience

CellPress
OPEN ACCESS

Article

Highly transmissible cytoplasmic incompatibility by the extracellular insect symbiont *Spiroplasma*

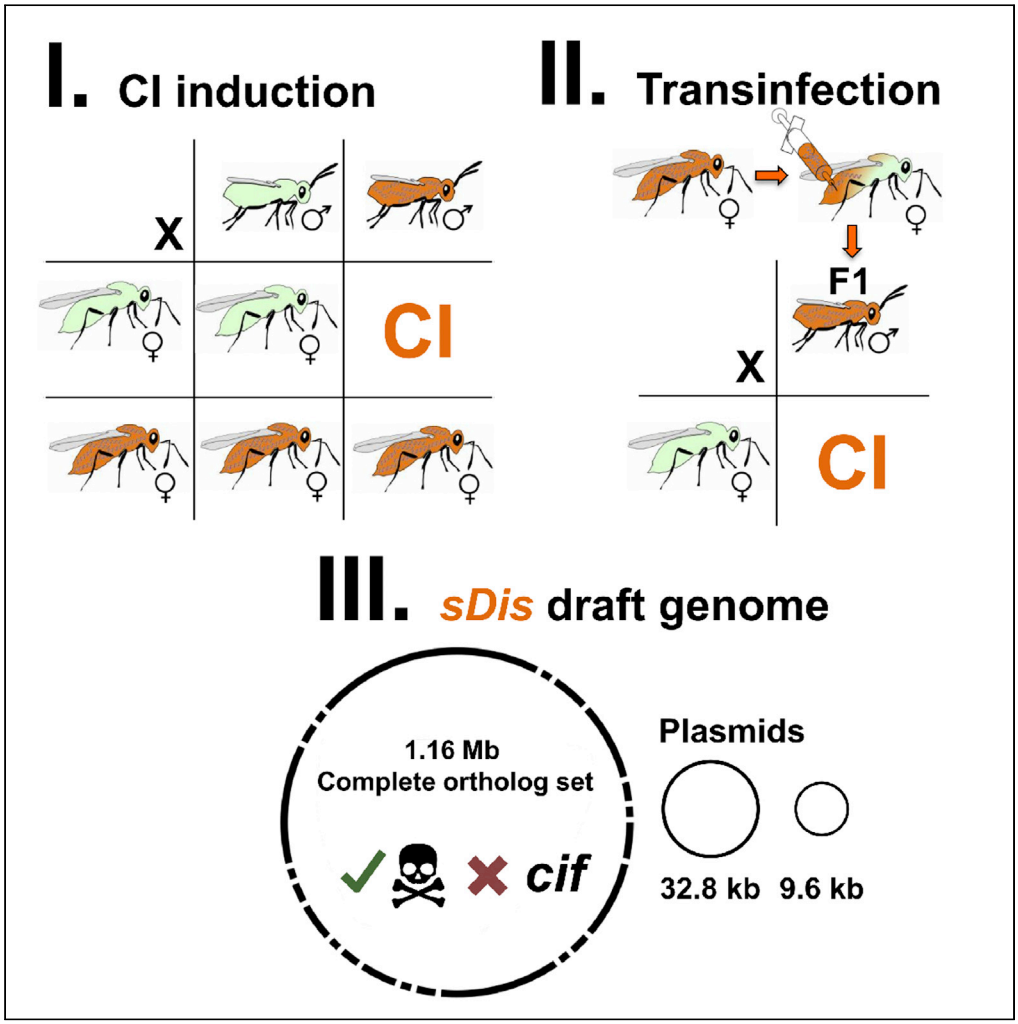

Marie Pollmann, Logan D. Moore, Elena Krimmer, ..., Matthew J. Ballinger, Johannes L.M. Steidle, Yuval Gottlieb

jsteidle@uni-hohenheim.de

Highlights

A *Spiroplasma* strain induces cytoplasmic incompatibility (CI) in a parasitoid wasp

Spiroplasma and CI are efficiently transferred to naive hosts by hemolymph injection

The CI-*Spiroplasma* genome contains potential CI-causing genes, but no *Wolbachia cifs*

Absence of *cif* genes in the *Spiroplasma* genome suggests an independent origin of CI

Pollmann et al., iScience *25*, 104335
May 20, 2022
https://doi.org/10.1016/j.isci.2022.104335

iScience

CellPress
OPEN ACCESS

Article

Highly transmissible cytoplasmic incompatibility by the extracellular insect symbiont *Spiroplasma*

Marie Pollmann,[1,9] Logan D. Moore,[2,9] Elena Krimmer,[3] Paul D'Alvise,[4] Martin Hasselmann,[5] Steve J. Perlman,[6] Matthew J. Ballinger,[2] Johannes L.M. Steidle,[1,7,10,*] and Yuval Gottlieb[8]

SUMMARY

Cytoplasmic incompatibility (CI) is a form of reproductive manipulation caused by maternally inherited endosymbionts infecting arthropods, like *Wolbachia*, whereby matings between infected males and uninfected females produce few or no offspring. We report the discovery of a new CI symbiont, a strain of *Spiroplasma* causing CI in the parasitoid wasp *Lariophagus distinguendus*. Its extracellular occurrence enabled us to establish CI in uninfected adult insects by transferring *Spiroplasma*-infected hemolymph. We sequenced the CI-*Spiroplasma* genome and did not find any homologues of any of the *cif* genes discovered to cause CI in *Wolbachia*, suggesting independent evolution of CI. Instead, the genome contains other potential CI-causing candidate genes, such as homologues of high-mobility group (HMG) box proteins that are crucial in eukaryotic development but rare in bacterial genomes. *Spiroplasma*'s extracellular nature and broad host range encompassing medically and agriculturally important arthropods make it a promising tool to study CI and its applications.

INTRODUCTION

A number of maternally transmitted microorganisms in arthropods have evolved the remarkable ability to manipulate their hosts' reproduction, in order to increase the frequency of infected hosts (Engelstädter and Hurst, 2009; Moran et al., 2008). The most common of these manipulations is cytoplasmic incompatibility (CI), whereby uninfected females produce few or no offspring upon mating with infected males (Shropshire et al., 2020; Werren, 1997). As a result, infected females have a significant advantage over their uninfected counterparts and can rapidly spread and replace them in the population (Shropshire et al., 2020; Werren, 1997).

In an important advance, the genetic basis of CI was recently discovered in the best studied CI microbe, the Alphaproteobacterium *Wolbachia pipientis*, and involves two linked genes, termed *cifA* and *cifB* (for cytoplasmic incompatibility factor). They operate in a manner similar to toxin-antitoxin systems, with one or both *cif* genes modifying or poisoning infected male sperm, and *cifA* alone rescuing incompatibility in the eggs of infected females (Adams et al., 2021; Beckmann et al., 2017; LePage et al., 2017). Without *cifA* rescue, paternally derived chromosomes are destroyed, resulting in embryonic lethality (Beckmann et al., 2017) (or haploid male development in some species with haplodiploid sex determination [Vavre et al., 2001]).

There is great interest in using CI microbes to control arthropod pests and disease vectors. This can be done in two ways, both of which involve establishing a new, stable CI infection in the target host species (Brelsfoard and Dobson, 2009). First, analogous to sterile insect techniques, large quantities of infected incompatible males can be released in the field, which will result in population crashes due to their mating with wild uninfected females (Brelsfoard and Dobson, 2009). Alternatively, CI microbes can be used to spread desired traits when females and males infected with a novel CI microbe are released in the wild (Brelsfoard and Dobson, 2009). This approach has been proven highly successful in reducing the prevalence of dengue virus in humans by releasing *Aedes aegypti* mosquitoes infected with a strain of the bacterial symbiont *Wolbachia* that causes both CI and suppresses viruses (Hoffmann et al., 2011; Utarini et al., 2021). *Wolbachia*-infected mosquitoes reach high frequencies due to CI, and this results in reduced dengue virus titer and transmission (Walker et al., 2011).

[1]Department of Chemical Ecology 190t, Institute of Biology, University of Hohenheim, 70599 Stuttgart, Germany

[2]Department of Biological Sciences, Mississippi State University, Mississippi State, MS 39762, USA

[3]Department of Animal Ecology and Tropical Biology, Biocenter, University of Wuerzburg, 97074 Wuerzburg, Germany

[4]Institute of Medical Microbiology and Hygiene, University Hospital of Tuebingen, 72016 Tuebingen, Germany

[5]Department of Livestock Population Genomics 460h, Institute of Animal Science, University of Hohenheim, 70599 Stuttgart, Germany

[6]Department of Biology, University of Victoria, Victoria, BC V8W 3N5, Canada

[7]KomBioTa - Center of Biodiversity and Integrative Taxonomy, University of Hohenheim, 70599 Stuttgart, Germany

[8]Koret School of Veterinary Medicine, Robert H. Smith Faculty of Agriculture, Food and Environment, Hebrew University of Jerusalem, POB 12, Rehovot 76100, Israel

[9]These authors contributed equally

[10]Lead contact

*Correspondence: jsteidle@uni-hohenheim.de

https://doi.org/10.1016/j.isci.2022.104335

Wolbachia is by far the best known and most common CI-inducing microbe. It was first shown to cause CI in *Culex pipientis* mosquitoes in the 1970s and has since been found to cause CI in at least 10 arthropod orders. In 2003, a second unrelated bacterial symbiont, *Candidatus* Cardinium hertigii (hereafter referred to as *Cardinium*), in the Bacteroidetes, was found to cause CI in a parasitic wasp (Hunter et al., 2003), with later studies extending this phenomenon to mites (Gotoh et al., 2007), planthoppers (Nakamura et al., 2012), and thrips (Nguyen et al., 2017). Although *Cardinium*-induced CI also involves modification of male sperm and rescue in females, sequencing its genome revealed that it does not contain homologues of the *Wolbachia cif* genes (Penz et al., 2012), indicating independent evolution of CI. More recently, a new bacterium in the same family as *Wolbachia*, called *Candidatus* Mesenet longicola (hereafter referred to as *Mesenet*), and a strain of the Gammaproteobacterium *Rickettsiella* were shown to cause CI in a beetle and a spider, respectively, but so far, little is known about them and the CI they induce (Rosenwald et al., 2020; Shropshire et al., 2020; Takano et al., 2017, 2021).

Here, we report the discovery of a surprising new CI microbe that infects *Lariophagus distinguendus* (Förster 1841) (Hymenoptera: Pteromalidae), a cosmopolitan parasitic wasp that is commonly used in biological control of beetle pests of stored products. Recently, we reported CI in *L. distinguendus*, marked by the absence of diploid female offspring in incompatible crosses (König et al., 2019). Interestingly, we detected neither *Wolbachia* nor *Cardinium* in wasps from the incompatible line (König et al., 2019).

Unexpectedly, we show that CI in *L. distinguendus* is caused by a maternally transmitted strain of *Spiroplasma*, a diverse lineage of microbes in the Gram-positive Mollicutes that includes pathogens and commensals, as well as several vertically transmitted endosymbionts, and infects a wide range of invertebrates (Gasparich, 2002; Regassa and Gasparich, 2006). Some vertically transmitted *Spiroplasma* produce female-biased sex ratios as male killers, whereas others protect their hosts against parasitic nematodes, wasps, and pathogenic fungi (Gasparich, 2002; Regassa and Gasparich, 2006).

Spiroplasma's localization in the hemolymph throughout host life facilitates rapid and efficient transfer of heritable infections to new hosts in the laboratory (Anbutsu and Fukatsu, 2011; Ballinger and Perlman, 2019). Indeed, we were able to transfer *Spiroplasma* and its CI phenotype to uninfected wasps using microinjection. This easy transferability and broad host range promise new possibilities for research into CI and its applications. Finally, we sequenced the genome of CI-inducing *Spiroplasma*. It contains no homologues of the *Wolbachia cif* genes, demonstrating a different genetic basis underlying *Spiroplasma*-induced CI. Instead, the genome harbors a number of interesting candidate genes, including novel toxins, genes containing ankyrin repeat domains, and eukaryotic high-mobility group (HMG) box proteins.

RESULTS

Bacteria induce CI in *L. distinguendus*

Tetracycline-treated and untreated females and males of the STU strain of *L. distinguendus* were crossed in all possible combinations, and offspring production was compared. Crosses between tetracycline-treated females and untreated males produced significantly fewer daughters ($p < 1 \times 10^{-4}$ *** in single comparisons with all other combinations, GLM, family = negative binomial, followed by Tukey test for multiple comparisons) and more sons ($p < 0.001$ *** in single comparisons with all other combinations, GLM, family = negative binomial, followed by Tukey test for multiple comparisons) with no difference in total offspring numbers ($p > 0.05$ n.s. in single comparisons with all other combinations, GLM, family = negative binomial, followed by Tukey test for multiple comparisons), which is indicative of the presence of CI-inducing bacteria (Figure 1, for full test statistics see Table S1). Increased male production is common in CI in hosts with haplodiploid sex determination, with incompatible fertilized embryos developing into males (Vavre et al., 2001).

Spiroplasma is the only reproductive manipulator

Individual wasps were tested for endosymbionts known to act as reproductive manipulators using PCR. Previously, we showed that the STU strain is not infected with either *Wolbachia* or *Cardinium* (König et al., 2019). Here, we also screened for *Rickettsia*, *Arsenophonus*, *Mesenet*, and *Rickettsiella*, as well as *Spiroplasma*. All tested STU females (n = 10) and 90% of the tested STU males (n = 10) were found to carry *Spiroplasma*, hereafter referred to as *sDistinguendus* (*sDis*); none of the other symbionts were present. In order to reveal a potential involvement of other bacteria, we used 16S rRNA amplicon sequencing of the whole bacterial community in five separate pooled samples of STU females. Overall, we found 12 amplicon sequence variants (ASVs), of which only five were present in at least four of the five samples

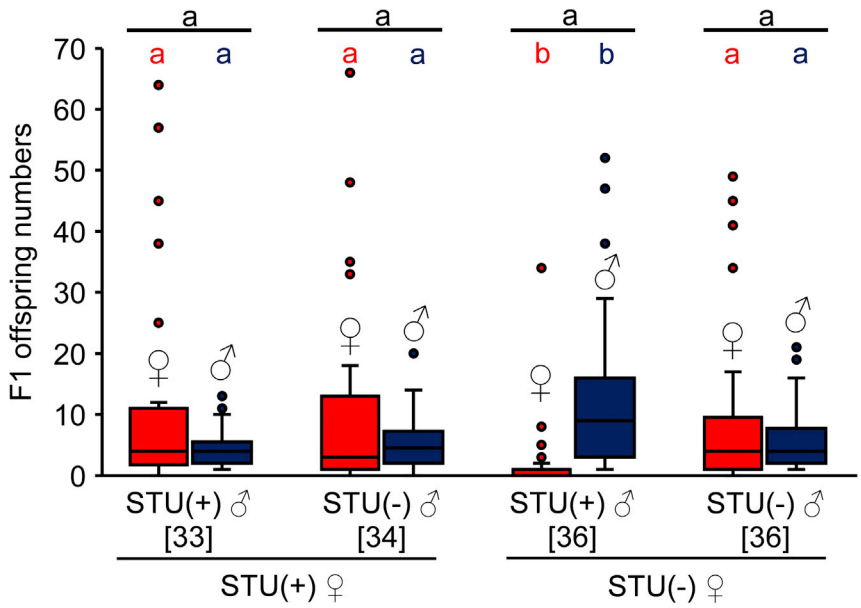

Figure 1. Numbers of F1 female (red) and male (blue) offspring of crosses between endosymbiont-carrying (+) and uninfected (−) females and males of the STU strain

Numbers of replicates (i.e the numbers of crosses) are given in parentheses below the paternal male of each combination. Statistical significances among numbers of female offspring, numbers of male offspring, and total offspring numbers, respectively, were tested using GLMs (family = negative binomial) followed by Tukey tests for multiple comparisons; different lower case letters (red: female offspring, blue: male offspring, black: total offspring) indicate statistical differences at $p < 0.05$ (see Table S1 for test statistics). Medians are represented by the middle horizontal lines; the 25% and 75% quartiles are shown as the lower and upper boundaries of the boxes, respectively. Minimum and maximum values within a range across 1.5 times the distances between the quartiles above the 75% quartile and below the 25% quartile are included in the whiskers; outliers outside of this range are shown as single points; see Data S1 for raw data.

sequenced. One ASV was identified as *Spiroplasma* and was present in all samples with an average of 8,258.4 total reads. Three ASVs were members of the Proteobacteria: a strain of *Yersinia* (4/5 samples, average of 22.6 total reads), a strain of *Pseudomonas* (4/5 samples, an average of 20.6 total reads), and an unidentified member of the Enterobacteriaceae (5/5 samples, average of 8411.6 total reads). The role of the unknown Enterobacteriaceae in CI was dismissed, as the rate of infection did not differ between tetracycline-treated (n = 5, 100% infection) and untreated (n = 4, 75% infection) STU females as well as CI-inducing (n = 4, 100% infection) and non-CI-inducing (n = 3, 100% infection) STU males (2x4 Fisher's Exact Test for Count Data, $p = 0.6875$). A standard nucleotide BLASTn (Altschul et al., 1990) of the consensus sequence resulted in many close hits of the same rank (Table S3) and a comparison with only the NCBI rRNA/ITS database found *Enterobacter cancerogenus*, for which a resistance to tetracycline has been shown before (Zwenger et al., 2008), to be the best match (99% coverage, 99.53% identity, E value = 0.0, GenBank: NR_044977.1).

The final ASV was identified as *Enterococcus* (phylum Firmicutes) with an average of 138.6 total reads (see Table 1 for full ASV count table). As *sDis* was the dominant bacterium and only potential reproductive manipulator, we set about characterizing it and establishing its role in CI.

sDis is present in the ovaries of *L. distinguendus*

To determine the presence of *sDis* in wasp ovaries, we performed fluorescent *in situ* hybridization (FISH) using the *Spiroplasma*-specific probe SPR and anti-sense and no-probe controls. Specific, localized signals were obtained with SPR in the ovaries of STU females (Figure 2).

sDis can be transferred to a noninfected host and induce CI

To demonstrate that the CI phenotype is ultimately induced by *sDis*, we performed a transinfection experiment. As a prerequisite, hemolymph from STU females was tested for infection with *sDis*. For the

Table 1. ASV count table from the NGS analysis of the microbiome of the *L. distinguendus* strain STU. See Table S3 for BLASTn matches to the 16S rRNA sequence of the Enterobacteriaceae

Total # of reads	Average # of reads	Class	Order	Family	Genus	Species
42,058	8411.6	Gammaproteobacteria	Enterobacteriales	Enterobacteriaceae	N/A	N/A
41,292	8258.4	Mollicutes	Entomoplasmatales	Spiroplasmataceae	*Spiroplasma*	secondary
693	138.6	Bacilli	Lactobacillales	Enterococcaceae	*Enterococcus*	N/A
113	22.6	Gammaproteobacteria	Enterobacteriales	Enterobacteriaceae	*Yersinia*	N/A
103	20.6	Gammaproteobacteria	Pseudomonadales	Pseudomonadaceae	*Pseudomonas*	N/A
12	2.4	Bacilli	Bacillales	Bacillaceae	N/A	N/A
11	2.2	Gammaproteobacteria	Pseudomonadales	Pseudomonadaceae	*Pseudomonas*	N/A
10	2	Alphaproteobacteria	Rhodobacterales	Rhodobacteraceae	*Rubellimicrobium*	N/A
6	1.2	Bacilli	Lactobacillales	Lactobacillaceae	*Lactobacillus*	N/A
4	0.8	Actinobacteria	Micrococcales	Micrococcaceae	N/A	N/A
4	0.8	Actinobacteria	Micrococcales	Brevibacteriaceae	*Brevibacterium*	N/A
2	0.4	Bacteroidia	Flavobacteriales	Flavobacteriaceae	*Flavobacterium*	resistens

transinfection, hemolymph from STU females was injected into endosymbiont-free STU(−) females. Of these, 27 (69.2%) were positive for *sDis* at the end of the experiment. These females were consecutively offered different batches of koi pellets infested with host beetle larvae to parasitize for two to three days each. The first three host batches parasitized by positive females produced *sDis*-negative offspring. Positive males started to emerge from the fourth batch and increased in proportion up to 100% in the last two batches (Figure 3A). Eventually, 15 of the positive injected females (56%) were found to have *sDis*-positive F1 male offspring.

Newly hatched F1 male offspring of injected females were mated to endosymbiont-free STU(−) females, and the presence of CI was inferred from the number of F2 females and F2 males. *sDis*-positive F1 males (n = 82) sired significantly fewer F2 females than uninfected F1 males (n = 36) (Wilcoxon rank-sum test with continuity correction, $W = 2{,}718$; $p = 3.581 \times 10^{-13}$ ***; Figure 3B), whereas the number of F2 male offspring was significantly higher in crosses with positive F1 males (Wilcoxon rank-sum test with continuity correction, $W = 839$, $p = 0.0001971$ ***), and total F2 offspring number did not differ between the crosses (Welch two sample t test, $t = 1.341$, $p = 0.1853$ n.s.) (Figure 3B), recreating the CI phenotype shown by Figure 1. This demonstrated that CI was induced by *sDis* and that *sDis* could be transferred into previously uninfected wasps by injection of hemolymph from infected wasps, maintaining its CI-inducing effect.

In order to examine whether the strength of CI was influenced by *Spiroplasma* titer, we conducted qPCR on the DNA samples of mated *sDis*-positive F1 male offspring of receiver females using *dnaA* as a target gene. There was no correlation between *Spiroplasma* titer in F1 male wasps and proportion of female offspring (number of female F2 offspring divided by total number of F2 offspring) used as proxy for CI level (Spearman's rank correlation, n = 36, rho = 0.171, $p = 0.319$)).

Genome of *sDis*

To explore the genetic basis of *sDis*-induced CI, we sequenced total genomic DNA extracted from adult *L. distinguendus* strain STU to 30x coverage (Figure S1). Phylogenomic analysis supported the position of *sDis* within an understudied *Spiroplasma* group, the Ixodetis clade, which is the most basal of the *Spiroplasma* clades (Gasparich et al., 2004) and includes strains that induce male killing in diverse insect hosts, including butterflies (Jiggins et al., 2000; Tabata et al., 2011) and beetles (Hurst et al., 1999; Majerus et al., 1999; Tinsley and Majerus, 2006) (Figure 4A).

Genome completeness was estimated at 96% based on the presence of all but five conserved single-copy Mollicutes orthologs in the BUSCO database. We searched manually for the missing orthologs and identified near-complete ORFs encoding four: *recA*, *rlmB*, *rplL*, and *metS*. We did not find a putative homologue of the remaining gene, *rsmI*, an rRNA ribose-2′-*O*-methyltransferase, in *sDis* or in any other Ixodetis clade *Spiroplasma* genome. Although this gene has a conserved role in bacterial translation, it appears to have been lost in this clade. Thus, the 96% BUSCO estimate is an underestimate. The draft assembly is

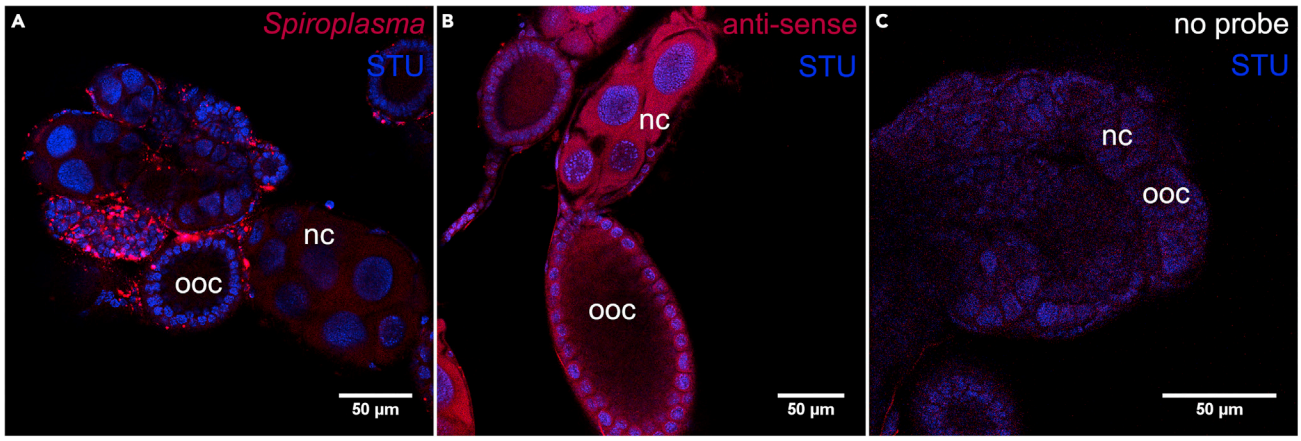

Figure 2. FISH images depicting the presence of *sDis* in the ovaries of *L. distinguendus* females of the strain STU

Blue: cell nuclei stained with Hoechst DNA staining, Red: *Spiroplasma*-specific probe (SPR) or anti-sense probe with Cy3 fluorochrome, nc: nurse cells, ooc: oocyte. Scale bars: 50 µm. Brightness and contrast were set to "auto" in ImageJ 1.x for all images.

(A) Specific, localized signals in STU ovaries hybridized with SPR.

(B) Background fluorescence in STU ovaries with anti-sense probe.

(C) Fluorescence of STU ovaries with no probe.

1.16 Mb in length and includes two closed plasmids (Table S6). Intact and pseudogenized insertion sequence transposes are abundant, comprising about 7.3% of the draft assembly. Of 1,175 predicted protein-coding genes, 462 could be assigned functional predictions in the form of KEGG numbers. Additional assembly statistics are presented in comparison to recently sequenced Ixodetis clade *Spiroplasma* in Table 2.

The s*Dis* symbiont encodes complete ATP synthase and glycolysis pathways, as well as transport components for glucose, fructose, GlcNAc, glycerol, and possibly mannose (Figure 5). Amino acid and lipid biosynthesis pathways are incomplete or absent, as reported previously for hemolymph-dwelling *Spiroplasma* species, including those in the Ixodetis clade (Martin et al., 2020; Vera-Ponce León et al., 2021; Yeoman et al., 2019). Incomplete pathway components were identified for lysine (*dapE*), valine, leucine, and isoleucine (*ilvA*), and arginine (*OTC*) synthesis. In addition to the PTS genes for carbon import, ABC membrane proteins for transport of phosphate (*ptsABCS*), nucleosides (bmpA, *nupABC*), and micronutrients (*ecfA1A2T*) could be identified. A comparative summary of membrane transport, biosynthesis, and metabolism genes in *sDis* and two other Ixodetis clade genomes is present in Table S4.

Known CI-related genes are absent from *sDis*

We searched the *sDis* genome for potential homologues of the *Wolbachia* CI genes (i.e. *cifA* and *cifB*), as well as the *Spiroplasma* male killing toxin gene *spaid* and the candidate *Wolbachia* male killing gene *wmk*. We did not find any *cif, spaid*, or *wmk* gene homologues. We found two OTUs and two PDDEXK genes that contained domains associated with type V cifB-like proteins, but closer investigation revealed only distant homology to the domains found in CI-inducers. Specifically, the OTU cysteine proteases of *sDis* are related to OTU domains of other *Spiroplasma* strains, while *Wolbachia cifB* OTU domains are in a different clade, and cluster with some *Rickettsia*, *Occidentia*, and *Mesenet* OTU domains (Figure S3, see Table S5 for a summary of search results for bacterial toxins and manipulation factors).

Candidate manipulation genes and virulence factors

Genome annotation and targeted tBLASTn searches revealed numerous symbiont genes with potential to impact key host structures and processes including development regulation, protein translation, protein degradation, and cell membrane integrity. The genome encodes four eukaryotic high-mobility group (HMG) box proteins. HMG1–3 bear domain similarity to HMG box proteins in the SOX-TCF family of DNA binding transcription factors that play crucial roles in embryonic development (Figure 4B). HMG2, 3, and 4 are found on small contigs (< 2000 bp), whereas HMG1 is present on a 25 kbp unclosed plasmid-like contig (MAEJMCOA_7; Table S6). HMG1 and the genes flanking it share greater sequence similarity with other Ixodetis clade *Spiroplasma* and with spirochetes than with Apis and Citri clade

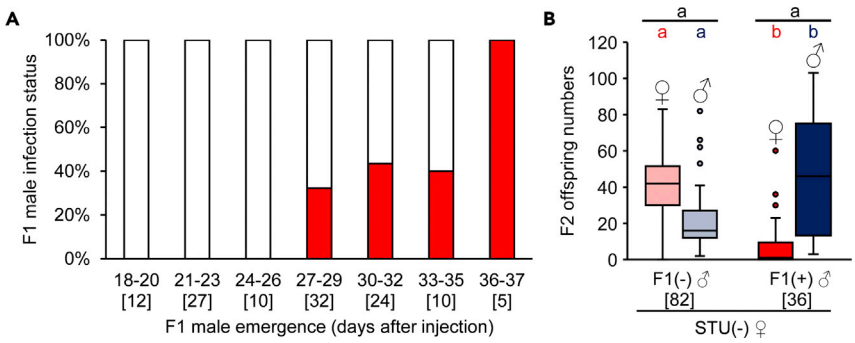

Figure 3. Hemolymph transfer of *sDis* infection and CI

(A) Proportion of *sDis*-positive F1 male offspring of injected females by day of emergence from consecutively parasitized host batches. Only males used for subsequent crossing experiments are shown. Numbers of replicates (numbers of males emerged in the respective time frame) are given in parentheses below the bars. White part of the bars: *sDis*-negative males; red part of the bars: *sDis*-positive males.

(B) Numbers of F2 female (red) and male (blue) offspring of *sDis*-negative (–) and positive (+) F1 males and uninfected (–) STU females. Numbers of replicates (numbers of males of the given infection status used for this experiment) are given in parentheses below the bars; crosses without any offspring are excluded. Statistical significances between crosses were tested for F2 female offspring and F2 male offspring using Wilcoxon rank sum tests with continuity correction ($W = 2718$, $p = 3.581 \times 10^{-13}$ for females, $W = 839$, $p = 0.0001971$ for males) and for F2 total offspring using a Welch two sample t test ($t = 1.341$, $p = 0.1853$); different lower case letters (red: female offspring, blue: male offspring, black: total offspring) indicate statistical differences at $p < 0.05$. The middle horizontal line shows the median; the lower boundary of the box indicates the 25% quartile, whereas the upper boundary represents the 75% quartile. The whiskers indicate minimum and maximum values within a range stretching from 1.5 times the distances between the quartiles above the 75% quartile and below the 25% quartile. Data outside of this range are outliers and are shown as single points. See Data S2 and Data S3 for raw data and *Spiroplasma* titers.

Spiroplasma. Flanking genes include plasmid partitioning and replication genes, conjugation proteins, insertion sequence elements, and uncharacterized proteins (Table S6).

We identified two translation-targeting toxins: a ribosome-inactivating protein (RIP) and a putative tRNA-inactivating nucleotidyltransferase distantly related to type IV abortive infection systems and absent from almost all other *Spiroplasma* (Cai et al., 2020) (Figure S3). RIPs have been implicated in *Spiroplasma*-mediated protection against natural enemies (Hamilton et al., 2016). We also identified one gene related to a pore-forming ETX/MTX2 toxin (Figure S3). Ankyrin repeat domains were identified in twelve genes (Figure S4). Several *sDis* ankyrin genes share similarities with *Wolbachia* and *Cardinium* genes (Table S6). Two *sDis* proteins contain OTU-like cysteine protease domains. This protease is one of three functional domains in the male killing *Spiroplasma* toxin, *spaid* (Harumoto and Lemaitre, 2018), although neither of the *sDis* domains bears strong amino acid sequence similarity to the *spaid* domain (Figure S3). One of the two OTU domains is closely related to homologues in the Ixodetis clade *Spiroplasma* symbionts of *Danaus chrysippus* and *Dactylopius coccus*, whereas the second is phylogenetically separate. The latter is present within a large hypothetical protein (957 aa) and is predicted to have a C-terminal domain with structural homology to staphopain and staphostatin, a cysteine protease and cysteine protease inhibitor from *Staphylococcus sp.*, respectively.

DISCUSSION

In this study, we demonstrate that the widespread symbiotic bacterium *Spiroplasma* causes cytoplasmic incompatibility in an insect host and show that the symbiont and phenotype can be efficiently transmitted by adult recipients following hemolymph microinjection. The benefits of understanding and applying CI have motivated decades of studies developing and optimizing protocols for symbiont transfer.

Prior to the present study, all CI-inducing bacteria have been primarily intracellular symbionts. There have been successful transfers of *Wolbachia* using hemolymph injection (Frydman, 2007), but most transinfections of CI-inducing symbionts require challenging techniques and specialized equipment for transfer into very young recipient embryos, often with limited success (Duplouy et al., 2013; Hughes and Rasgon, 2014; Walker et al., 2011; Xi et al., 2005; Zabalou et al., 2004).

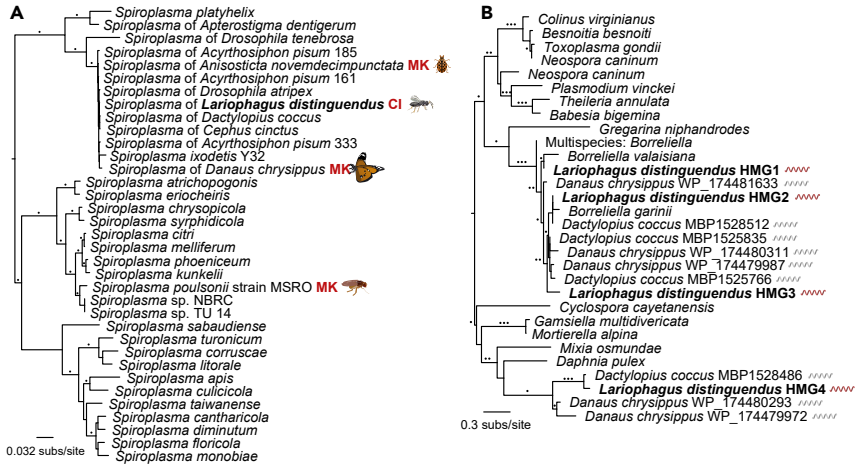

Figure 4. Evolutionary relationships of the CI-inducing *sDis*

(A) Maximum likelihood phylogram of concatenated *rpoB*, *16S rRNA*, and *23S rRNA* nucleotide sequences supports the phylogenetic position of the novel symbiont within the Ixodetis clade of *Spiroplasma*. Branches with 100% ML-like FastTree support are labeled with a small filled circle. Resolved phylogenomic relationships within Ixodetis clade members are shown in Figure S2.

(B) Phylogenetic relationships between eukaryotic and *Spiroplasma*-encoded high-mobility group (HMG) box proteins. Two well-supported clades of *Spiroplasma* HMG box proteins are identified and distantly allied with fungal and protist HMG box proteins. One clade is interspersed with spirochete-encoded proteins. All *Spiroplasma* genes are indicated by gray or red (*sDis*) helical cartoons, and *sDis* genes are additionally shown in bold typeface. Branches with ML-like FastTree support values of 0.75 or greater are labeled with a small filled circle; two circles indicate support > 0.8 and three indicate support > 0.9.

Spiroplasma's ecology as a hemolymph-dwelling bacterium bypasses all of these challenges.

In our study system, we were able to establish CI-*Spiroplasma* by adult-to-adult microinjection, mirroring previous results showing high success of *Spiroplasma* transfer between fruit fly hosts using this method (Ballinger and Perlman, 2019; Haselkorn and Jaenike, 2015). Our horizontal transfer experiments also suggest that the strength of CI in *Spiroplasma* is not related to overall bacterial titer, which also has positive implications for the success of transferring CI to new hosts.

As a new phenotype for *Spiroplasma*, this discovery presents exciting new avenues for basic and applied research in arthropod reproductive manipulation. Like other facultative symbionts, *Spiroplasma* has a broad host range that does not reflect host or symbiont phylogeny (Binetruy et al., 2019; Gasparich et al., 2004). Closely related *Spiroplasma* Ixodetis clade strains infect fruit flies, aphids, ticks, sawflies, scale insects, and spiders. Reproductive manipulations performed by members of this group can also affect many different arthropod hosts, as evident by the male killing strains in butterflies and beetles (Hurst et al., 1999; Jiggins et al., 2000; Majerus et al., 1999; Tabata et al., 2011; Tinsley and Majerus, 2006)—and now a CI strain in wasps. This broad host manipulation range suggests a potential for the transfer and maintenance of *sDis* to diverse arthropod hosts of agricultural, medical, and basic research relevance that should be a focus of future studies. Beyond the Ixodetis clade, the host range of *Spiroplasma* is even broader, with strains infecting terrestrial and aquatic arthropods [Regassa and Gasparich, 2006; Wang et al., 2011]), jellyfish (Cortés-Lara et al., 2015), and sea cucumbers (He et al., 2018). If the ease of *Spiroplasma* transfer can be replicated for interspecific transfers of *sDis* as well, it will facilitate similar investigations of *sDis*'s reproductive effects in other insect hosts. Finally, a number of *Spiroplasma* strains, including vertically transmitted male killers, can be grown in cell-free media and genetically transformed (Masson et al., 2018, 2020), which has the potential to greatly facilitate the study and manipulation of CI.

The discovery that *Spiroplasma* can cause CI adds to a growing list of microbial symbionts, such as *Rickettsiella* and *Mesenet*, that join *Wolbachia* and *Cardinium* in the small club of CI microbes. As infection with multiple symbionts is common, this suggests that if we observe CI, we should be careful not to assume that it is being caused by *Wolbachia*. However, it is possible to use differing susceptibility to antibiotics to link CI to a specific symbiont; for example, *Wolbachia* is highly susceptible to rifampicin, whereas *Spiroplasma* is resistant (Jaenike et al., 2010).

Table 2. Genome assembly statistics of the CI-*Spiroplasma* and related symbionts

Genome	Size (bp)	Contigs	%GC	N50	CDS	tRNAs	Ref
Spiroplasma of *Lariophagus distinguendus*	1,163,832	198	24.3	14,219	1,175	27	—
Spiroplasma of *Cephus cinctus*	713,566	145	24.9	5,160	754	23	(Yeoman et al., 2019)
Spiroplasma of *Danaus chrysippus*	1,745,430	12	23.7	215,399	1,782	27	(Martin et al., 2020)
Spiroplasma of *Dactylopius coccus* (DCF)	1,195,508	286	23.7	6,014	1,253	27	(Vera-Ponce León et al., 2021)
Spiroplasma poulsonii strain MSRO[a,b]	1,883,005	1	26.4	Closed	2,217	31	(Masson et al., 2018; Paredes et al., 2015)

[a]Male killing strain.
[b]Citri clade.

The *sDis* genome provides a first look at gene candidates potentially involved in *Spiroplasma* CI. The notable absence of *cif* homologues mirrors observations from the genome of CI-*Cardinium*, suggesting independent evolution of CI. It is striking that the cytological phenotype of CI is similar in both *Wolbachia* and *Cardinium* despite being caused by the expression of different genes, suggesting a convergent development to affect the same targets in the hosts (Gebiola et al., 2017; Mann et al., 2017; Penz et al., 2012). Although it is possible that some *sDis* genes are missing from our draft assembly, we note that our genome is more complete than the 96% estimate obtained by BUSCO analysis, as four of the five missing genes could be identified by manual BLAST and the last is absent from all Ixodetis clade *Spiroplasma* genomes sequenced to date. Identification of eukaryotic HMG box DNA-binding proteins in *sDis* may be of interest given the shared chromatin-bridging phenotype in these other systems. For example, in *Drosophila melanogaster*, HMG box-like proteins play a crucial role in chromatin condensing during spermatogenesis (Doyen et al., 2015; Rathke et al., 2010). Interestingly, depletion of maternally provided chromatin decondensing proteins during fertilization results in complete sterility in *Drosophila*. With the exception of spirochetes, homologous HMG genes are rare in bacteria, yet we identified gene families in *sDis* as well as two closely related *Spiroplasma* symbionts, including the male killing symbiont of *D. chrysippus*. Indeed, it is interesting that closely related *Spiroplasma* Ixodetis clade strains cause male killing and CI, as previous studies have demonstrated a close link between CI and male killing in *Wolbachia*. For example, multiple *Wolbachia* CI-inducing strains have been shown to act as male killers following introgression into different host genetic backgrounds (Jaenike, 2007; Sasaki et al., 2002, 2005).

The *sDis* genome also encodes genes with a collection of protein domains, such as OTU-like cysteine proteases and ankyrin repeats, that are present in *spaid*, the toxin that causes male killing in *Spiroplasma poulsonii* (Harumoto and Lemaitre, 2018). Both the *cif*s and *spaid* are evolutionarily dynamic genes—with *cif*s being widespread and rapidly evolving components of WO prophage regions in *Wolbachia* genomes (LePage et al., 2017; Lindsey et al., 2018) and *spaid* being plasmid-encoded (Masson et al., 2018). In this context, plasmid-encoded genes may be the strongest candidates for CI in *sDis*. The two closed plasmids and two additional candidate plasmids of *sDis* encode an HMG box protein and ankyrin-domain-containing proteins, as well as numerous hypothetical proteins absent functional predictions. A common feature of facultative symbiont genomes and those of *Spiroplasma* especially is an abundance of uncharacterized protein coding genes (Duplouy et al., 2013; Paredes et al., 2015; Siozios et al., 2019). Nearly half of the predicted genes of *sDis* lack functional annotations based on their amino acid sequences. Future studies will be crucial to identify further gene candidates and characterize their role in this new CI system.

Limitations of the study

We successfully transferred *Spiroplasma* and the CI it induces to uninfected *Lariophagus* wasp hosts via hemolymph injection. A critical next step will be to determine the potential host range of this strain of *Spiroplasma*, along with its ability to induce CI, by attempting to establish infections in different and more distantly related host species. Also, although our nearly complete *sDis* draft genome suggests several CI candidate genes and an independently evolved route to CI, the function of these candidates and their potential role in CI have not yet been tested. In addition, further sequencing is required to close the *sDis* assembly and confirm its completeness.

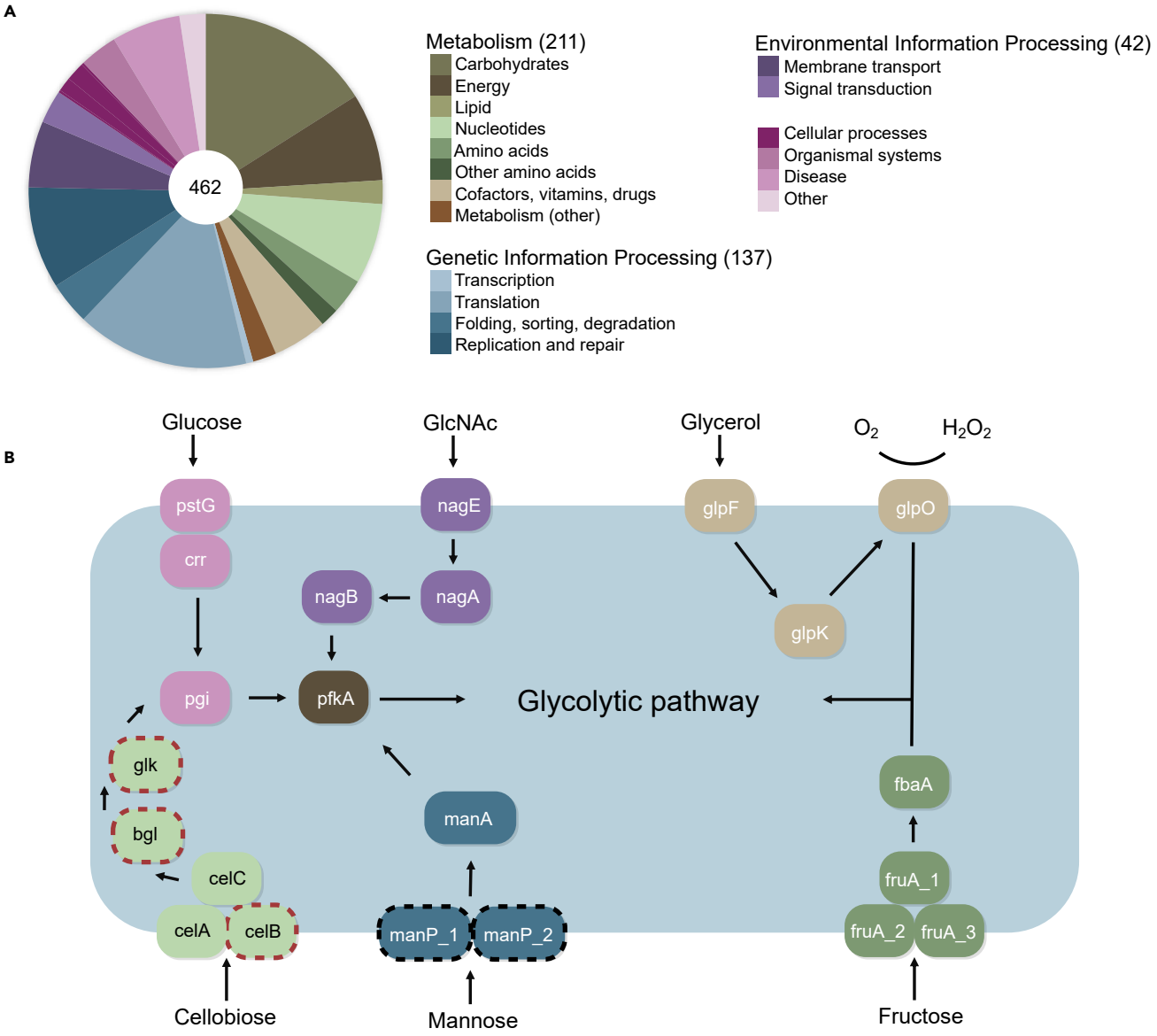

Figure 5. Gene content and putative carbon utilization in *sDis*

(A) Summary of gene content in the *sDis* genome assembly organized by function as predicted by matches to KEGG gene databases. Numbers in the center of the chart and beside category headings indicate numbers of genes.

(B) Summary of putative carbon utilization by *sDis*. Complete coding regions corresponding to each named gene are present in the assembly. Dashed black outlines indicate multifunctional genes whose functions are not confidently predicted based on presence. Dashed red lines indicate genes that are absent from the assembly. Color schemes are not shared across panels (A) and (B).

STAR★METHODS

Detailed methods are provided in the online version of this paper and include the following:

- KEY RESOURCES TABLE
- RESOURCE AVAILABILITY
  - Lead contact
  - Materials availability
  - Data and code availability
- EXPERIMENTAL MODEL AND SUBJECT DETAILS

SUPPLEMENTAL INFORMATION

Supplemental information can be found online at https://doi.org/10.1016/j.isci.2022.104335.

ACKNOWLEDGMENTS

MP and EK were financially supported by the Ministry for Science, Research and the Arts of Baden-Württemberg as part of the partnership fund of the Robert H. Smith Faculty of Agriculture, Food and Environment of the Hebrew University of Jerusalem (HUJI) in Rehovot and the Faculties of Agricultural and Natural Sciences of the University of Hohenheim (UHOH) to JLMS and YG. The authors would like to thank Einat Kapri and Maya Lalzar for conducting some of the experiments. SJP acknowledges funding support from a Sinergia grant from the Swiss National Science Foundation (grant no. CRSII3_154396) and from the Discovery Grant program of the Natural Sciences and Engineering Research Council of Canada. MJB is supported in part by a Center of Biomedical Research Excellence grant from the National Institute of General Medical Sciences (Grant P20 GM103646) of the National Institutes of Health.

AUTHOR CONTRIBUTIONS

MP and LDM performed research, analyzed data, and wrote the paper; EK and PDA performed research and analyzed data; MH, MJB, JLMS, and YG designed research; SJP designed research and wrote the paper.

DECLARATION OF INTERESTS

The authors declare no competing interests.

Received: January 24, 2022
Revised: April 6, 2022
Accepted: April 26, 2022
Published: May 20, 2022

SUPPORTING CITATIONS

The following reference appears in the Supplemental Information: Benson et al., 2012; Massey and Newton, 2021

REFERENCES

Adams, K.L., Abernathy, D.G., Willett, B.C., Selland, E.K., Itoe, M.A., and Catteruccia, F. (2021). *Wolbachia cifB* induces cytoplasmic incompatibility in the malaria mosquito vector. Nat. Microbiol. *6*, 1575–1582. https://doi.org/10.1038/s41564-021-00998-6.

Altschul, S.F., Gish, W., Miller, W., Myers, E.W., and Lipman, D.J. (1990). Basic local alignment search tool. J. Mol. Biol. *215*, 403–410. https://doi.org/10.1016/S0022-2836(05)80360-2.

Amann, R.I., Binder, B.J., Olson, R.J., Chisholm, S.W., Devereux, R., and Stahl, D.A. (1990). Combination of 16S rRNA-targeted oligonucleotide probes with flow cytometry for analyzing mixed microbial populations. Appl. Environ. Microbiol. *56*, 1919–1925. https://doi.org/10.1128/aem.56.6.1919-1925.1990.

Anbutsu, H., and Fukatsu, T. (2011). *Spiroplasma* as a model insect endosymbiont. Environ. Microbiol. Rep. *3*, 144–153. https://doi.org/10.1111/j.1758-2229.2010.00240.x.

Ballinger, M.J., and Perlman, S.J. (2019). The defensive *Spiroplasma*. Curr. Opin. Insect

Sci. *32*, 36–41. https://doi.org/10.1016/j.cois.2018.10.004.

Bankevich, A., Nurk, S., Antipov, D., Gurevich, A.A., Dvorkin, M., Kulikov, A.S., Lesin, V.M., Nikolenko, S.I., Pham, S., Prjibelski, A.D., et al. (2012). SPAdes: a new genome assembly algorithm and its applications to single-cell sequencing. J. Comput. Biol. *19*, 455–477. https://doi.org/10.1089/cmb.2012.0021.

Beckmann, J.F., Ronau, J.A., and Hochstrasser, M. (2017). A *Wolbachia* deubiquitylating enzyme induces cytoplasmic incompatibility. Nat. Microbiol. *2*, 17007. https://doi.org/10.1038/nmicrobiol.2017.7.

Benson, D.A., Karsch-Mizrachi, I., Clark, K., Lipman, D.J., Ostell, J., and Sayers, E.W. (2012). Genbank. Nucleic Acids Res. *40*, D48–D53. https://doi.org/10.1093/nar/gkr1202.

Binetruy, F., Bailly, X., Chevillon, C., Martin, O.Y., Bernasconi, M.V., and Duron, O. (2019). Phylogenetics of the *Spiroplasma ixodetis* endosymbiont reveals past transfers between ticks and other arthropods. Ticks Tick Borne Dis. *10*, 575–584. https://doi.org/10.1016/j.ttbdis.2019.02.001.

Brelsfoard, C.L., and Dobson, S.L. (2009). *Wolbachia*-based strategies to control insect pests and disease vectors. Asia Pac. J. Mol. Biol. Biotechnol. *17*, 55–63.

Bushnell, B. (2014). BBMap: a fast, accurate, splice-aware aligner. https://www.osti.gov/servlets/purl/1241166.

Cai, Y., Usher, B., Gutierrez, C., Tolcan, A., Mansour, M., Fineran, P.C., Condon, C., Neyrolles, O., Genevaux, P., and Blower, T.R. (2020). A nucleotidyltransferase toxin inhibits growth of *Mycobacterium tuberculosis* through inactivation of tRNA acceptor stems. Sci. Adv. *6*, eabb6651. https://doi.org/10.1126/sciadv.abb6651.

Callahan, B.J., McMurdie, P.J., Rosen, M.J., Han, A.W., Johnson, A.J.A., and Holmes, S.P. (2016). DADA2: high-resolution sample inference from Illumina amplicon data. Nat. Methods *13*, 581–583. https://doi.org/10.1038/nmeth.3869.

Cortés-Lara, S., Urdiain, M., Mora-Ruiz, M., Prieto, L., and Rosselló-Móra, R. (2015). Prokaryotic microbiota in the digestive cavity of the jellyfish *Cotylorhiza tuberculata*. Syst. Appl. Microbiol. *38*, 494–500. https://doi.org/10.1016/j.syapm.2015.07.001.

Dally, M., Lalzar, M., Belausov, E., Gottlieb, Y., Coll, M., and Zchori-Fein, E. (2020). Cellular localization of two *Rickettsia* symbionts in the digestive system and within the ovaries of the mirid bug, *Macrolophous pygmaeus*. Insects *11*, 530. https://doi.org/10.3390/insects11080530.

Doyen, C.M., Chalkley, G.E., Voets, O., Bezstarosti, K., Demmers, J.A., Moshkin, Y.M., and Verrijzer, C.P. (2015). A testis-specific chaperone and the chromatin remodeler ISWI mediate repackaging of the paternal genome. Cell Rep. *13*, 1310–1318. https://doi.org/10.1016/j.celrep.2015.10.010.

Duplouy, A., Iturbe-Ormaetxe, I., Beatson, S.A., Szubert, J.M., Brownlie, J.C., McMeniman, C.J., McGraw, E.A., Hurst, G.D.D., Charlat, S., O'Neill, S.L., et al. (2013). Draft genome sequence of the male-killing *Wolbachia* strain *w*Bol1 reveals recent horizontal gene transfers from diverse sources. BMC Genom. *14*, 20. https://doi.org/10.1186/1471-2164-14-20.

Duron, O., Cremaschi, J., and McCoy, K.D. (2016). The high diversity and global distribution of the intracellular bacterium *Rickettsiella* in the polar seabird tick *Ixodes uriae*. Microb. Ecol. *71*, 761–770. https://doi.org/10.1007/s00248-015-0702-8.

Engelstädter, J., and Hurst, G.D.D. (2009). The ecology and evolution of microbes that manipulate host reproduction. Annu. Rev. Ecol. Evol. Syst. *40*, 127–149. https://doi.org/10.1146/annurev.ecolsys.110308.120206.

Finn, R.D., Clements, J., and Eddy, S.R. (2011). HMMER web server: interactive sequence similarity searching. Nucleic Acids Res. *39*, W29–W37. https://doi.org/10.1093/nar/gkr367.

Fox, J., and Weisberg, S. (2019). An R companion to applied regression, third edition (Sage). https://socialsciences.mcmaster.ca/jfox/Books/Companion/.

Frank, J.A., Reich, C.I., Sharma, S., Weisbaum, J.S., Wilson, B.A., and Olsen, G.J. (2008). Critical evaluation of two primers commonly used for amplification of bacterial 16S rRNA genes. Appl. Environ. Microbiol. *74*, 2461–2470. https://doi.org/10.1128/AEM.02272-07.

Frydman, H. (2007). *Wolbachia* bacterial infection in *Drosophila*. J. Vis. Exp. *158*. https://doi.org/10.3791/158.

Fukatsu, T., Tsuchida, T., Nikoh, N., and Koga, R. (2001). *Spiroplasma* symbiont of the pea aphid, *Acyrthosiphon pisum* (Insecta: Homoptera). Appl. Environ. Microbiol. *67*, 1284–1291. https://doi.org/10.1128/AEM.67.3.1284-1291.2001.

Gasparich, G.E. (2002). Spiroplasmas: evolution, adaptation and diversity. Front. Biosci. *7*. d619–40. https://doi.org/10.2741/A799.

Gasparich, G.E., Whitcomb, R.F., Dodge, D., French, F.E., Glass, J., and Williamson, D.L. (2004). The genus *Spiroplasma* and its non-helical descendants: phylogenetic classification, correlation with phenotype and roots of the *Mycoplasma mycoides* clade. Int. J. Syst. Evol. Microbiol. *54*, 893–918. https://doi.org/10.1099/ijs.0.02688-0.

Gebiola, M., Giorgini, M., Kelly, S.E., Doremus, M.R., Ferree, P.M., and Hunter, M.S. (2017). Cytological analysis of cytoplasmic incompatibility induced by *Cardinium* suggests convergent evolution with its distant cousin *Wolbachia*. Proc. R. Soc. B *284*, 20171433. https://doi.org/10.1098/rspb.2017.1433.

Gotoh, T., Noda, H., and Ito, S. (2007). *Cardinium* symbionts cause cytoplasmic incompatibility in spider mites. Heredity *98*, 13–20. https://doi.org/10.1038/sj.hdy.6800881.

Gottlieb, Y., Ghanim, M., Chiel, E., Gerling, D., Portnoy, V., Steinberg, S., Tzuri, G., Horowitz, A.R., Belausov, E., Mozes-Daube, N., et al. (2006). Identification and localization of a *Rickettsia* sp. in *Bemisia tabaci* (Homoptera: Aleyrodidae). Appl. Environ. Microbiol. *72*, 3646–3652. https://doi.org/10.1128/AEM.72.5.3646-3652.2006.

Grubbs, F.E. (1950). Sample criteria for testing outlying observations. Ann. Math. Statist. *21*, 27–58. https://doi.org/10.1214/aoms/1177729885.

Hamilton, P.T., Peng, F., Boulanger, M.J., and Perlman, S.J. (2016). A ribosome-inactivating protein in a *Drosophila* defensive symbiont. Proc. Natl. Acad. Sci. U S A *113*, 350–355. https://doi.org/10.1073/pnas.1518648113.

Harumoto, T., and Lemaitre, B. (2018). Male-killing toxin in a bacterial symbiont of *Drosophila*. Nature *557*, 252–255. https://doi.org/10.1038/s41586-018-0086-2.

Haselkorn, T.S., and Jaenike, J. (2015). Macroevolutionary persistence of heritable endosymbionts: acquisition, retention and expression of adaptive phenotypes in *Spiroplasma*. Mol. Ecol. *24*, 3752–3765. https://doi.org/10.1111/mec.13261.

He, L.-S., Zhang, P.-W., Huang, J.-M., Zhu, F.-C., Danchin, A., and Wang, Y. (2018). The enigmatic genome of an obligate ancient *Spiroplasma* symbiont in a hadal holothurian. Appl. Environ. Microbiol. *84*. e01965–17. https://doi.org/10.1128/AEM.01965-17.

Hoffmann, A.A., Montgomery, B.L., Popovici, J., Iturbe-Ormaetxe, I., Johnson, P.H., Muzzi, F., Greenfield, M., Durkan, M., Leong, Y.S., Dong, Y., et al. (2011). Successful establishment of *Wolbachia* in *Aedes* populations to suppress dengue transmission. Nature *476*, 454–457. https://doi.org/10.1038/nature10356.

Holehouse, K.A., Hammond, R.L., and Bourke, A.F.G. (2003). Non-lethal sampling of DNA from bumble bees for conservation genetics. Insectes Soc. *50*, 277–285. https://doi.org/10.1007/s00040-003-0672-6.

Hothorn, T., Bretz, F., and Westfall, P. (2008). Simultaneous inference in general parametric models. Biom. J. *50*, 346–363. https://doi.org/10.1002/bimj.200810425.

Hughes, G.L., and Rasgon, J.L. (2014). Transinfection: a method to investigate *Wolbachia*–host interactions and control arthropod-borne disease. Insect Mol. Biol. *23*, 141–151. https://doi.org/10.1111/imb.12066.

Hunter, M.S., Perlman, S.J., and Kelly, S.E. (2003). A bacterial symbiont in the Bacteroidetes induces cytoplasmic incompatibility in the parasitoid wasp *Encarsia pergandiella*. Proc. R. Soc. B *270*, 2185–2190. https://doi.org/10.1098/rspb.2003.2475.

Hurst, G.D.D., Jiggins, F.M., Schulenburg, J.H.G.v.d., Bertrand, D., West, S.A., Goriacheva, I.I., Zakharov, I.A., Werren, J.H., Stouthamer, R., and Majerus, M.E.N. (1999). Male–killing *Wolbachia* in two species of insect. Proc. R. Soc. B *266*, 735–740. https://doi.org/10.1098/rspb.1999.0698.

Jaenike, J. (2007). Spontaneous emergence of a new *Wolbachia* phenotype. Evolution *61*, 2244–2252. https://doi.org/10.1111/j.1558-5646.2007.00180.x.

Jaenike, J., Unckless, R., Cockburn, S.N., Boelio, L.M., and Perlman, S.J. (2010). Adaptation via symbiosis: recent spread of a *Drosophila*

defensive symbiont. Science *329*, 212–215. https://doi.org/10.1126/science.1188235.

Jiang, P., Green, S.J., Chlipala, G.E., Turek, F.W., and Vitaterna, M.H. (2019). Reproducible changes in the gut microbiome suggest a shift in microbial and host metabolism during spaceflight. Microbiome *7*, 113. https://doi.org/10.1186/s40168-019-0724-4.

Jiggins, F.M., Hurst, G.D.D., Jiggins, C.D., Schulenburg, J.H.G.v.d., and Majerus, M.E.N. (2000). The butterfly *Danaus chrysippus* is infected by a male-killing *Spiroplasma* bacterium. Parasitology *120*, 439–446. https://doi.org/10.1017/S0031182099005867.

Kanehisa, M., Sato, Y., and Morishima, K. (2016). BlastKOALA and GhostKOALA: KEGG tools for functional characterization of genome and metagenome sequences. J. Mol. Biol. *428*, 726–731. https://doi.org/10.1016/j.jmb.2015.11.006.

Katoh, K., and Standley, D.M. (2013). MAFFT multiple sequence alignment software version 7: improvements in performance and usability. Mol. Biol. Evol. *30*, 772–780. https://doi.org/10.1093/molbev/mst010.

König, K., Zundel, P., Krimmer, E., König, C., Pollmann, M., Gottlieb, Y., and Steidle, J.L.M. (2019). Reproductive isolation due to prezygotic isolation and postzygotic cytoplasmic incompatibility in parasitoid wasps. Ecol. Evol. *9*, 10694–10706. https://doi.org/10.1002/ece3.5588.

Laczny, C.C., Kiefer, C., Galata, V., Fehlmann, T., Backes, C., and Keller, A. (2017). BusyBee Web: metagenomic data analysis by bootstrapped supervised binning and annotation. Nucleic Acids Res. *45*, W171–W179. https://doi.org/10.1093/nar/gkx348.

LePage, D.P., Metcalf, J.A., Bordenstein, S.R., On, J., Perlmutter, J.I., Shropshire, J.D., Layton, E.M., Funkhouser-Jones, L.J., Beckmann, J.F., and Bordenstein, S.R. (2017). Prophage WO genes recapitulate and enhance *Wolbachia*-induced cytoplasmic incompatibility. Nature *543*, 243–247. https://doi.org/10.1038/nature21391.

Lindsey, A.R.I., Rice, D.W., Bordenstein, S.R., Brooks, A.W., Bordenstein, S.R., and Newton, I.L.G. (2018). Evolutionary genetics of cytoplasmic incompatibility genes *cifA* and *cifB* in prophage WO of *Wolbachia*. Genome Biol. Evol. *10*, 434–451. https://doi.org/10.1093/gbe/evy012.

Madeira, F., Park, Y.M., Lee, J., Buso, N., Gur, T., Madhusoodanan, N., Basutkar, P., Tivey, A.R.N., Potter, S.C., Finn, R.D., and Lopez, R. (2019). The EMBL-EBI search and sequence analysis tools APIs in 2019. Nucleic Acids Res. *47*, W636–W641. https://doi.org/10.1093/nar/gkz268.

Majerus, T.M.O., Schulenburg, J.H.G.v.d., Majerus, M.E.N., and Hurst, G.D.D. (1999). Molecular identification of a male-killing agent in the ladybird *Harmonia axyridis* (Pallas) (Coleoptera: Coccinellidae). Insect Mol. Biol. *8*, 551–555. https://doi.org/10.1046/j.1365-2583.1999.00151.x.

Mann, E., Stouthamer, C.M., Kelly, S.E., Dzieciol, M., Hunter, M.S., and Schmitz-Esser, S. (2017). Transcriptome sequencing reveals novel candidate genes for *Cardinium hertigii*-caused cytoplasmic incompatibility and host-cell interaction. mSystems *2*. e00141–17. https://doi.org/10.1128/mSystems.00141-17.

Manske, M. (2006). GENtle, a free multi-purpose molecular biology tool. PhD thesis (University of Cologne). http://gentle.magnusmanske.de/.

Mapleson, D., Garcia Accinelli, G., Kettleborough, G., Wright, J., and Clavijo, B.J. (2017). KAT: a K-mer analysis toolkit to quality control NGS datasets and genome assemblies. Bioinformatics *33*, 574–576. https://doi.org/10.1093/bioinformatics/btw663.

Martin, S.H., Singh, K.S., Gordon, I.J., Omufwoko, K.S., Collins, S., Warren, I.A., Munby, H., Brattström, O., Traut, W., Martins, D.J., et al. (2020). Whole-chromosome hitchhiking driven by a male-killing endosymbiont. PLoS Biol. *18*, e3000610. https://doi.org/10.1371/journal.pbio.3000610.

Massey, J.H., and Newton, I.L.G. (2021). Diversity and function of arthropod endosymbiont toxins. Trends Microbiol. *30*, 185–198. https://doi.org/10.1016/j.tim.2021.06.008.

Masson, F., Calderon Copete, S., Schüpfer, F., Garcia-Arraez, G., and Lemaitre, B. (2018). *In vitro* culture of the insect endosymbiont *Spiroplasma poulsonii* highlights bacterial genes involved in host-symbiont interaction. mBio *9*. e00024–18. https://doi.org/10.1128/mBio.00024-18.

Masson, F., Schüpfer, F., Jollivet, C., and Lemaitre, B. (2020). Transformation of the *Drosophila* sex-manipulative endosymbiont *Spiroplasma poulsonii* and persisting hurdles for functional genetic studies. Appl. Environ. Microbiol. *86*. e00835–20. https://doi.org/10.1128/AEM.00835-20.

Moran, N.A., McCutcheon, J.P., and Nakabachi, A. (2008). Genomics and evolution of heritable bacterial symbionts. Annu. Rev. Genet. *42*, 165–190. https://doi.org/10.1146/annurev.genet.41.110306.130119.

Nakamura, Y., Yukuhiro, F., Matsumura, M., and Noda, H. (2012). Cytoplasmic incompatibility involving *Cardinium* and *Wolbachia* in the white-backed planthopper *Sogatella furcifera* (Hemiptera: Delphacidae). Appl. Entomol. Zool. *47*, 273–283. https://doi.org/10.1007/s13355-012-0120-z.

Nguyen, D.T., Morrow, J.L., Spooner-Hart, R.N., and Riegler, M. (2017). Independent cytoplasmic incompatibility induced by *Cardinium* and *Wolbachia* maintains endosymbiont coinfections in haplodiploid thrips populations. Evolution *71*, 995–1008. https://doi.org/10.1111/evo.13197.

Nishimura, O., Hara, Y., and Kuraku, S. (2017). GVolante for standardizing completeness assessment of genome and transcriptome assemblies. Bioinformatics *33*, 3635–3637. https://doi.org/10.1093/bioinformatics/btx445.

Paredes, J.C., Herren, J.K., Schüpfer, F., Marin, R., Claverol, S., Kuo, C.-H., Lemaitre, B., and Bevén, L. (2015). Genome sequence of the *Drosophila melanogaster* male-killing *Spiroplasma* strain MSRO endosymbiont. mBio *6*. e02437–14. https://doi.org/10.1128/mBio.02437-14.

Penz, T., Schmitz-Esser, S., Kelly, S.E., Cass, B.N., Müller, A., Woyke, T., Malfatti, S.A., Hunter, M.S., and Horn, M. (2012). Comparative genomics suggests an independent origin of cytoplasmic incompatibility in *Cardinium hertigii*. PLoS Genet. *8*, e1003012. https://doi.org/10.1371/journal.pgen.1003012.

Price, M.N., Dehal, P.S., and Arkin, A.P. (2010). FastTree 2 - approximately maximum-likelihood trees for large alignments. PLoS One *5*, e9490. https://doi.org/10.1371/journal.pone.0009490.

Quast, C., Pruesse, E., Yilmaz, P., Gerken, J., Schweer, T., Yarza, P., Peplies, J., and Glöckner, F.O. (2013). The SILVA ribosomal RNA gene database project: improved data processing and web-based tools. Nucleic Acids Res. *41*, D590–D596. https://doi.org/10.1093/nar/gks1219.

R Core Team (2020). R: a language and environment for statistical computing (R Foundation for Statistical Computing). https://www.R-project.org/.

Rathke, C., Barckmann, B., Burkhard, S., Jayaramaiah-Raja, S., Roote, J., and Renkawitz-Pohl, R. (2010). Distinct functions of Mst77F and protamines in nuclear shaping and chromatin condensation during *Drosophila* spermiogenesis. Eur. J. Cell Biol. *89*, 326–338. https://doi.org/10.1016/j.ejcb.2009.09.001.

Regassa, L.B., and Gasparich, G.E. (2006). Spiroplasmas: evolutionary relationships and biodiversity. Front. Biosci. *11*, 2983–3002. https://doi.org/10.2741/2027.

Rosenwald, L.C., Sitvarin, M.I., and White, J.A. (2020). Endosymbiotic *Rickettsiella* causes cytoplasmic incompatibility in a spider host. Proc. R. Soc. B *287*, 20201107. https://doi.org/10.1098/rspb.2020.1107.

RStudio Team (2020). RStudio: integrated development for R. RStudio (Boston, MA: RStudio, Inc.). https://www.rstudio.com/.

Sasaki, T., Kubo, T., and Ishikawa, H. (2002). Interspecific transfer of *Wolbachia* between two lepidopteran insects expressing cytoplasmic incompatibility: a *Wolbachia* variant naturally infecting *Cadra cautella* causes male killing in *Ephestia kuehniella*. Genetics *162*, 1313–1319. https://doi.org/10.1093/genetics/162.3.1313.

Sasaki, T., Massaki, N., and Kubo, T. (2005). *Wolbachia* variant that induces two distinct reproductive phenotypes in different hosts. Heredity *95*, 389–393. https://doi.org/10.1038/sj.hdy.6800737.

Schneider, C.A., Rasband, W.S., and Eliceiri, K.W. (2012). NIH Image to ImageJ: 25 years of image analysis. Nat. Methods *9*, 671–675. https://doi.org/10.1038/nmeth.2089.

Seemann, T. (2014). Prokka: rapid prokaryotic genome annotation. Bioinformatics *30*, 2068–2069. https://doi.org/10.1093/bioinformatics/btu153.

Shropshire, J.D., Leigh, B., and Bordenstein, S.R. (2020). Symbiont-mediated cytoplasmic incompatibility: what have we learned in 50 years? eLife *9*, e61989. https://doi.org/10.7554/eLife.61989.

Simão, F.A., Waterhouse, R.M., Ioannidis, P., Kriventseva, E.V., and Zdobnov, E.M. (2015). BUSCO: assessing genome assembly and annotation completeness with single-copy

orthologs. Bioinformatics *31*, 3210–3212. https://doi.org/10.1093/bioinformatics/btv351.

Siozios, S., Pilgrim, J., Darby, A.C., Baylis, M., and Hurst, G.D.D. (2019). The draft genome of strain cCpun from biting midges confirms insect *Cardinium* are not a monophyletic group and reveals a novel gene family expansion in a symbiont. PeerJ *7*, e6448. https://doi.org/10.7717/peerj.6448.

Tabata, J., Hattori, Y., Sakamoto, H., Yukuhiro, F., Fujii, T., Kugimiya, S., Mochizuki, A., Ishikawa, Y., and Kageyama, D. (2011). Male killing and incomplete inheritance of a novel *Spiroplasma* in the moth *Ostrinia zaguliaevi*. Microb. Ecol. *61*, 254–263. https://doi.org/10.1007/s00248-010-9799-y.

Takano, S.-I., Gotoh, Y., and Hayashi, T. (2021). "*Candidatus* Mesenet longicola": novel endosymbionts of *Brontispa longissima* that induce cytoplasmic incompatibility. Microb. Ecol. *82*, 512–522. https://doi.org/10.1007/s00248-021-01686-y.

Takano, S.-I., Tuda, M., Takasu, K., Furuya, N., Imamura, Y., Kim, S., Tashiro, K., Iiyama, K., Tavares, M., and Amaral, A.C. (2017). Unique clade of alphaproteobacterial endosymbionts induces complete cytoplasmic incompatibility in the coconut beetle. Proc. Natl. Acad. Sci. U S A *114*, 6110–6115. https://doi.org/10.1073/pnas.1618094114.

Thao, M.L., and Baumann, P. (2004). Evidence for multiple acquisition of *Arsenophonus* by whitefly species (Sternorrhyncha: Aleyrodidae). Curr. Microbiol. *48*, 140–144. https://doi.org/10.1007/s00284-003-4157-7.

Tinsley, M.C., and Majerus, M.E.N. (2006). A new male-killing parasitism: *Spiroplasma* bacteria infect the ladybird beetle *Anisosticta novemdecimpunctata* (Coleoptera: Coccinellidae). Parasitology *132*, 757–765. https://doi.org/10.1017/S0031182005009789.

Utarini, A., Indriani, C., Ahmad, R.A., Tantowijoyo, W., Arguni, E., Ansari, M.R., Supriyati, E., Wardana, D.S., Meitika, Y., Ernesia, I., et al. (2021). Efficacy of *Wolbachia*-infected mosquito deployments for the control of dengue. N. Engl. J. Med. *384*, 2177–2186. https://doi.org/10.1056/NEJMoa2030243.

Vavre, F., Dedeine, F., Quillon, M., Fouillet, P., Fleury, F., and Boulétreau, M. (2001). Within-species diversity of *Wolbachia*-induced cytoplasmic incompatibility in haplodiploid insects. Evolution *55*, 1710–1714. https://doi.org/10.1111/j.0014-3820.2001.tb00691.x.

Vera-Ponce León, A., Dominguez-Mirazo, M., Bustamante-Brito, R., Higareda-Alvear, V., Rosenblueth, M., and Martínez-Romero, E. (2021). Functional genomics of a *Spiroplasma* associated with the carmine cochineals *Dactylopius coccus* and *Dactylopius opuntiae*. BMC Genom. *22*, 240. https://doi.org/10.1186/s12864-021-07540-2.

Walker, T., Johnson, P.H., Moreira, L.A., Iturbe-Ormaetxe, I., Frentiu, F.D., McMeniman, C.J., Leong, Y.S., Dong, Y., Axford, J., Kriesner, P., et al. (2011). The wMel *Wolbachia* strain blocks dengue and invades caged *Aedes aegypti* populations. Nature *476*, 450–453. https://doi.org/10.1038/nature10355.

Walters, W., Hyde, E.R., Berg-Lyons, D., Ackermann, G., Humphrey, G., Parada, A., Gilbert, J.A., Jansson, J.K., Caporaso, J.G., Fuhrman, J.A., et al. (2016). Improved bacterial 16S rRNA gene (V4 and V4-5) and fungal internal transcribed spacer marker gene primers for microbial community surveys. mSystems *1*. e00009–15. https://doi.org/10.1128/mSystems.00009-15.

Wang, W., Gu, W., Gasparich, G.E., Bi, K., Ou, J., Meng, Q., Liang, T., Feng, Q., Zhang, J., and Zhang, Y. (2011). *Spiroplasma eriocheiris* sp. nov., associated with mortality in the Chinese mitten crab, *Eriocheir sinensis*. Int. J. Syst. Evol. Microbiol. *61*, 703–708. https://doi.org/10.1099/ijs.0.020529-0.

Weisburg, W.G., Barns, S.M., Pelletier, D.A., and Lane, D.J. (1991). 16S ribosomal DNA amplification for phylogenetic study. J. Bacteriol. *173*, 697–703. https://doi.org/10.1128/jb.173.2.697-703.1991.

Werren, J.H. (1997). Biology of *Wolbachia*. Annu. Rev. Entomol. *42*, 587–609. https://doi.org/10.1146/annurev.ento.42.1.587.

Wick, R.R., Judd, L.M., Gorrie, C.L., and Holt, K.E. (2017). Unicycler: resolving bacterial genome assemblies from short and long sequencing reads. PLoS Comput. Biol. *13*, e1005595. https://doi.org/10.1371/journal.pcbi.1005595.

Xi, Z., Dean, J.L., Khoo, C., and Dobson, S.L. (2005). Generation of a novel *Wolbachia* infection in *Aedes albopictus* (Asian tiger mosquito) via embryonic microinjection. Insect Biochem. Mol. Biol. *35*, 903–910. https://doi.org/10.1016/j.ibmb.2005.03.015.

Yeoman, C.J., Brutscher, L.M., Esen, Ö.C., Ibaoglu, F., Fowler, C., Eren, A.M., Wanner, K., and Weaver, D.K. (2019). Genome-resolved insights into a novel *Spiroplasma* symbiont of the wheat stem sawfly (*Cephus cinctus*). PeerJ *7*, e7548. https://doi.org/10.7717/peerj.7548.

Zabalou, S., Riegler, M., Theodorakopoulou, M., Stauffer, C., Savakis, C., and Bourtzis, K. (2004). *Wolbachia*-induced cytoplasmic incompatibility as a means for insect pest population control. Proc. Natl. Acad. Sci. U S A *101*, 15042–15045. https://doi.org/10.1073/pnas.0403853101.

Zimmermann, L., Stephens, A., Nam, S.-Z., Rau, D., Kübler, J., Lozajic, M., Gabler, F., Söding, J., Lupas, A.N., and Alva, V. (2018). A completely reimplemented MPI bioinformatics toolkit with a new HHpred server at its core. J. Mol. Biol. *430*, 2237–2243. https://doi.org/10.1016/j.jmb.2017.12.007.

Zwenger, S.R., Welsch, T., and Gillock, E.T. (2008). Bacteria resistant to ciprofloxacin, chloramphenicol and tetracycline isolated from western Kansas feedlots. Trans. Kans. Acad. Sci. *111*, 125–135. https://doi.org/10.1660/0022-8443(2008)111[125:BRTCCA]2.0.CO;2.

STAR★METHODS

KEY RESOURCES TABLE

REAGENT or RESOURCE	SOURCE	IDENTIFIER
Chemicals, peptides, and recombinant proteins		
Tetracycline hydrochloride	Sigma-Aldrich Chemie GmbH, Taufkirchen, Germany	Cat#87130
molecular biology grade proteinase K	Sigma-Aldrich Products Ltd., Rehovot, Israel	Cat#3115887001
IGEPAL®CA-630	Sigma-Aldrich Products Ltd., Rehovot, Israel	Cat#I8896
Critical commercial assays		
nexttec™ 1-Step DNA Isolation Kit for Tissue & Cells	nexttec Biotechnologie GmbH, Hilgertshausen, Germany	Cat#10N.050
DNeasy® Blood & Tissue Kit	QIAGEN LLC, Germantown MD, USA	Cat#69504
GoTaq®Green Master Mix 2X	Promega, Madison WI, USA	Cat#M7122
Green GoTaq® Reaction Buffer	Promega, Madison WI, USA	Cat#M7911
dNTPs	Promega, Madison WI, USA	Cat#U1330
GoTaq® G2 DNA Polymerase	Promega, Madison WI, USA	Cat#M7841
ROTI®Pol TaqS Red-Mix (2x)	Carl Roth GmbH + Co. KG, Karlsruhe, Germany	Cat#9241.1
peqGREEN	VWR International GmbH, Darmstadt, Germany	Cat#732-3196
RedSafe™ Nucleic Acid Staining Solution	iNtRON Biotechnology, Inc.	Cat#21141
LowRanger 100 bp DNA	Norgen Biotek Corp., Canada	Cat#11500
equimolar 100 bp ladder	Carl Roth GmbH + Co. KG, Karlsruhe, Germany	Cat#T834.1
GeneJet Gel extraction and DNA Cleanup Micro Kit	Thermo Fisher Scientific, Waltham MA, USA	Cat#K0831
pGEM®-T Easy Vector kit	Promega, Madison WI, USA	Cat#1380
peqGold Plasmid Miniprep Kit I	VWR International GmbH, Darmstadt, Germany	Cat#12-6942-1
Platinum® SYBR® Green qPCR SuperMix-UDG	Invitrogen, Carlsbad CA, USA	Cat#11733038
DreamTaq™ Green DNA Polymerase with DreamTaq™ Green Buffer	Thermo Fisher Scientific, Waltham MA, USA	Cat#EP0711
Oxford Nanopore MinION	Oxford Nanopore Technologies, Oxford Science Park, UK	Cat#Min101B
Ligation sequencing kit	Oxford Nanopore Technologies, Oxford Science Park, UK	Cat#SQK-LSK109
Deposited data		
NGS sequences	This paper	GenBank: OL684700-OL684711
Spiroplasma sp. sequence	This paper	GenBank: OM334830
Enterobacter sp. sequence	This paper	GenBank: OM273870
WGS sequences	This paper	NCBI BioProject: PRJNA826431
Experimental models: Organisms/strains		
Lariophagus distinguendus strain dbSTU-D1	Dept. of Chemical Ecology, University of Hohenheim	N/A
Oligonucleotides		
See Table S2 for list of primers	N/A	N/A
Fluorescent probe Eub338-Cy3 5′-Cy3-ACT CCT ACG GGA GGC AGC-3′	(Amann et al., 1990)	N/A

(*Continued on next page*)

Continued

REAGENT or RESOURCE	SOURCE	IDENTIFIER
Fluorescent probe SPR-Cy3 5′-Cy3-CCC ACC TTC CTC TAG CTT AC-3′	This study	N/A
Software and algorithms		
GENtle v. 1.9.4.	(Manske, 2006)	http://gentle.magnusmanske.de/
Axiovision 4.6	Carl Zeiss AG, Oberkochen, Germany	https://www.micro-shop.zeiss.com/en/us/system/software+axiovision-axiovision+program-axiovision+software/10221/
ImageJ 1.x	(Schneider et al., 2012)	https://imagej.nih.gov/ij/
GIMP v. 2.10.24	Kimball, Mattis and the GIMP Development Team	https://www.gimp.org/
R v. 4.0.3	(R Core Team, 2020)	https://www.R-project.org/
RStudio v. 1.3.1093	(RStudio Team, 2020)	https://www.rstudio.com/
multcomp v.14.-15, R package	(Hothorn et al., 2008)	http://multcomp.R-forge.R-project.org
car v. 3.0-10, R package	(Fox and Weisberg, 2019)	https://socialsciences.mcmaster.ca/jfox/Books/Companion/
dada2 v. 1.14.0, R package	(Callahan et al., 2016)	https://github.com/benjjneb/dada2/releases/tag/v1.14
BBMap	(Bushnell, 2014)	https://sourceforge.net/projects/bbmap/
SPAdes 3.10.1	(Bankevich et al., 2012)	https://github.com/ablab/spades
KAT	(Mapleson et al., 2017)	https://kat.readthedocs.io/en/latest/#
BUSCO	(Simão et al., 2015)	https://busco.ezlab.org/
gVolante	(Nishimura et al., 2017)	https://gvolante.riken.jp/
Prokka v 1.14.5	(Seemann, 2014)	https://github.com/tseemann/prokka
BLASTKoala	(Kanehisa et al., 2016)	https://www.kegg.jp/blastkoala/
BLAST	(Altschul et al., 1990)	https://blast.ncbi.nlm.nih.gov/Blast.cgi
MAFFT 7.388	(Katoh and Standley, 2013)	https://mafft.cbrc.jp/alignment/software/
Geneious Prime	Geneious 2022.0.1	https://www.geneious.com/
Unicycler	(Wick et al., 2017)	https://github.com/rrwick/Unicycler
FastTree 2.1.11	(Price et al., 2010)	http://microbesonline.org/fasttree/
HMMER 3.3	(Finn et al., 2011)	http://hmmer.org/

RESOURCE AVAILABILITY

Lead contact

Further information and requests for resources and reagents should be directed to and will be fulfilled by the lead contact, Johannes L.M. Steidle (jsteidle@uni-hohenheim.de).

Materials availability

This study did not generate new unique reagents.

Data and code availability

All data generated in this study will be publicly available as of the date of publication. Accession numbers for sequences submitted to the NCBI database are listed in the key resources table.

This paper does not report original code.

Any additional information required to reanalyze the data reported in this paper is available from the lead contact upon request.

EXPERIMENTAL MODEL AND SUBJECT DETAILS

Lariophagus distinguendus

In our experiments, we used the *L. distinguendus* strain dbSTU-D1 (STU), which was collected in households in 2007 in Stuttgart-Bad Cannstatt, Germany. The strain was reared on six-week-old larvae of *Stegobium paniceum* in koi pellets (Hikari Friend, Kamihata Fish Industry Group, Kyorin Corporation, Japan) in glass jars with a ventilated lid (diameter 12 cm, height 16 cm). Beetles were reared by placing about 1 g of newly emerged unsexed adult beetles (about 700 beetles) on 80 g koi pellets. After six weeks, freshly emerged *L. distinguendus* were placed on the infested pellets. The cultures were kept at 26 °C and 45% RH with a natural light:dark cycle. To obtain virgin wasps for the experiments, they were isolated in the pupal stage by dissecting the koi pellets and kept individually in 1.5 ml tubes until eclosion. An endosymbiont-free line, termed STU(-), was obtained by tetracycline treatment for at least three generations. Newly emerged wasps were placed in a Petri dish containing filter paper and a piece of cotton wool soaked in a solution of tetracycline (1 mg/ml) and sucrose (100 mg/ml). After 24 h, wasps were placed on host-infested substrate as described above. The loss of endosymbionts was confirmed by PCR (as described below) for randomly chosen individuals prior to using these lines in experiments.

METHOD DETAILS

Crossing experiments

1-day-old single virgin wasp males and females of the antibiotic and untreated lines were placed together to enable mating in all possible combinations. All pairs were subsequently transferred to host-infested substrate for oviposition, i.e. 5 g of koi pellets containing *S. paniceum* larvae. After 4 to 5 weeks, the number and sex of emerging offspring were recorded. Crossings without any offspring were excluded from the analysis.

Specific testing for bacteria

The wasps were tested for the presence of *Spiroplasma*, *Rickettsia*, *Arsenophonus*, *Mesenet*, and *Rickettsiella*. For the DNA extraction, two different methods were used. One method consisted of crushing single wasps in 10 µl of a lysis buffer (9.95 µl TE-buffer with 10mM Tris, 0.5 mM EDTA, 3 mg molecular biology grade proteinase K (Sigma-Aldrich Products Ltd., Rehovot, Israel), and 0.5 µl IGEPAL®CA-630 (Sigma-Aldrich Products Ltd., Rehovot, Israel)) and the subsequent incubation of the mixture with another 30 µl or 90 µl of the same buffer at 65°C for 15 min and 95°C for 10 min using a heating block. Alternatively, wasp DNA was extracted using the nexttec™ 1^{-Step} DNA Isolation Kit for Tissue & Cells (nexttec Biotechnologie GmbH, Hilgertshausen, Germany) following the corresponding protocol. The PCR conditions generally consisted of an initial denaturation step at 94 to 95°C for 1 to 4 min, 35 cycles of 92°C or 95°C for 30 s, 30 s at the respective annealing temperatures of 55 to 58°C and 30 to 60 s at 72°C followed by a final extension at 72°C for 5 min (see Table S2 for details). The reaction mix consisted either of 20 µl Promega GoTaq®Green Master Mix 2X (Promega, Madison WI, USA), with 4 µl of each primer and 10 µl of double distilled water per 2 µl sample, 5 µl Promega 5X Green GoTaq® Reaction Buffer with 0.5 µl 10mM dNTPs (Promega, Madison WI, USA), 1 µl of each primer, 16.375 µl double distilled water and 0.125 µl Promega GoTaq® G2 DNA Polymerase (Promega, Madison WI, USA) per 1 µl sample or 12.5 µl of ROTI®Pol TaqS Red-Mix (2x) (Carl Roth GmbH + Co. KG, Karlsruhe, Germany) with 1 µl of each primer and 9.5 µl of double distilled water per 1 µl sample. The PCRs were performed using a Biometra professional Basic Thermocycler (Analytik Jena AG, Jena, Germany), a Biometra TGradient 96 Thermocycler (Analytik Jena AG, Jena, Germany) or a Techne® Prime Thermocycler (Cole-Parmer, Stone, UK). Gel electrophoresis was conducted on a 1 to 2% agarose gel using 5 µl peqgreen (VWR International GmbH, Darmstadt, Germany) per 100 ml TAE buffer or 5 to 10 µl RedSafe™ Nucleic Acid Staining Solution (iNtRON Biotechnology, Inc.) for DNA staining and Norgen LowRanger 100 bp DNA (Norgen Biotek Corp., Canada) or an equimolar 100 bp ladder (Carl Roth GmbH + Co. KG, Karlsruhe, Germany) as ladder. Of each sample, 5 to 10 µl were transferred to the gel. All PCR experiments in this study followed these procedures unless stated otherwise. We used the primers ApDnaAF1 (5′-ATT CTT CAG TAA AAA TGC TTG GA-3′ (Fukatsu et al., 2001)) and ApDnaAR1 (5′-ACA CAT TTA CTT CAT GCT ATT GA-3′ (Fukatsu et al., 2001)) to test for *Spiroplasma*, and RB-F (5′-GCT CAG AAC GAA CGC TAT C-3′ (Gottlieb et al., 2006)) and RB-R (5′-GAA GGA AAG CAT CTC TGC -3′ (Gottlieb et al., 2006)), respectively, for *Rickettsia*. Ars23S-1(5′-CGT TTG ATG AAT TCA TAG TCA AA-3′ (Thao and Baumann, 2004)) and Ars23S-2 (5′-GGT CCT CCA GTT AGT GTT ACC CAA C-3′ (Thao and Baumann, 2004)) were used to test for *Arsenophonus*, L355F (5′-GCT ATG CCG CGT GAG TGA TT-3′ (Takano et al.,

2017)) and L749R (5′-ACA CAG AAA TAA AAA TTC CTA C-3′ (Takano et al., 2017)) for *Mesenet* and RLA16SF1 (5′-CAG TAA ARR TTT CGG YCT TTA YGG G-3′ (Duron et al., 2016)) and RLA16SR1 (5′-CAA ACC TAG TCA ACC ACC TAC ACG-3′ (Duron et al., 2016)) for *Rickettsiella*.

Next generation sequencing of the microbiome

The whole microbiome of the STU strain was subjected to Next Generation Sequencing (16S rRNA amplicon sequencing) with five samples consisting of 50 females each, following the procedure described by (Dally et al., 2020). DNA extraction was conducted using the DNeasy® Blood and Tissue kit (QIAGEN, Germantown, MD, USA) according to the manufacturer's instructions. PCR was conducted with the primer pair 515F (5′-GTG YCA GCM GCC GCG GTA A-3′)/926R (5′-CCG YCA ATT YMT TTR AGT TT-3′), targeting the V4-V5 variable regions of microbial 16S rDNA (Walters et al., 2016) to screen for microbes. Sequencing of the resulting amplicons was performed on an Illumina MiSeq sequencer (Illumina Inc., San Diego, CA) as described by (Jiang et al., 2019) using a MiSeq v3 flow cell (Illumina Inc., San Diego, CA). PCR, library preparation, and sequencing were performed at the University of Illinois at Chicago Sequencing Core (UICSQC).

The DADA2 pipeline, provided by the R package "dada2" (v. 1.14.0) (Callahan et al., 2016) was implemented to process the obtained sequences by trimming them and filtering those with poor quality ("filterAndTrim", maxEE = 2, maxN = 0 and trimleft = 15). Error rate was estimated ("learnErrors", randomize set to "TRUE") and corrected sequences were inferred with the dada2 algorithm ("dada"). Complete sequences were assembled from the forward and reverse sequences via "mergePairs" and chimeras were identified and removed ("removeBimeraDenovo"). A count table containing the amplicon sequence variants (ASVs) and their respective counts was created ("makeSequenceTable"). The taxonomic matches of the ASVs were determined via the "assignTaxonomy" command (minimum bootstrap confidence value at 80%) using the SILVA non-redundant small subunit ribosomal RNA database (v.132) (Quast et al., 2013) as reference, and added to the table for further analysis.

Testing for Enterobacteriaceae

Tetracycline-treated and untreated STU females, as well as STU males of both CI and non-CI crossings were tested for the Enterobacteriaceae detected by NGS using the primers 27f (5′-AGA GTT TGA TCC TGG CTC AG-3′ (Weisburg et al., 1991)), 1492r (5′-TAC CTT GTT ACG ACT T-3′ (Frank et al., 2008)), EnterobacterF (5′-GAG GGT GCA AGC GTT AAT CGG-3′), and EnterobacterR (5′-AGC GTC AGT CTT TGT CCA GGG-3′) (also see Table S2). A sample of a tetracycline-treated STU female subjected to PCR with the primer combination 27f/1492r was chosen for Sanger Sequencing and sent to Microsynth Seqlab (Göttingen, Germany) for this purpose. The sequence was processed with GENtle v. 1.9.4. (© by Magnus Manske, University of Cologne, released under GPL, 2003) (Manske, 2006).

Fluorescent *in-situ* hybridization

In order to test the presence of *Spiroplasma* in the ovaries of *L. distinguendus*, the ovipositor with attached ovaries of live females was removed in 1 x PBS using fine needles. Ovaries were kept in FAA (5% acetic acid, 5% formaldehyde, 90% absolute ethanol) for fixation for 1 to 3 days. The fixed ovaries were washed in 50% ethanol and successively incubated in fresh 50% ethanol, 80% ethanol and 100% ethanol for 15 min each. Afterwards, the ovaries were air-dried for 10 min and subsequently moved to hybridization buffer (20 mM pH 8.0 Tris-HCl, 0.9 M NaCl, 35% formamide, 0.01% SDS) pre-warmed at 46°C for an incubation period of 15 min. The hybridization buffer was then replaced by pre-warmed hybridization buffer containing the fluorescent probes. The *Spiroplasma*-specific probe SPR-Cy3 (5′-Cy3-CCC ACC TTC CTC TAG CTT AC-3′) and as controls the probe anti-sense Eub338-Cy3 (5′-Cy3-ACT CCT ACG GGA GGC AGC-3′ (Amann et al., 1990)), as well as a no-probe approach were used. The samples were incubated overnight at 46°C for hybridization. After incubation in 500 µl of pre-warmed washing buffer (20 mM Tris-HCl pH 8.0, 80 mM NaCl, 50 mM EDTA, 0.01% SDS) for 15 min, the samples were left in 1 ml of pre-warmed washing buffer for 30 min and subsequently washed twice with 1 x PBS. For mounting on a slide with 1 x PBS, the cuticles were removed from the ovaries, and a drop of mountant (glycerol, 1 x PBS, Hoechst staining) was added to the slide before it was covered with a coverslip that was fixed with nail polish. The slides were incubated in the dark for several minutes before being analyzed. Visual analysis was performed using a Zeiss LSM 700 confocal microscope (Carl Zeiss AG, Oberkochen, Germany) with an AxioCam HSm video camera (Carl Zeiss AG, Oberkochen, Germany) and Axiovision 4.6 software (Carl Zeiss AG, Oberkochen, Germany).

ImageJ 1.x (Schneider et al., 2012) and the GNU Image Manipulation Program (GIMP, v. 2.10.24, © Spencer Kimball, Peter Mattis and the GIMP Development Team, www.gimp.org) were applied for processing.

Transinfection experiments

Transinfection experiments were performed to study if CI can be induced in an endosymbiont-free strain by infection with *Spiroplasma*. Hemolymph was transferred from infected female wasps (donor females) to uninfected STU(-) females (receiver females). Male offspring of receiver females were mated to endosymbiont-free females to check for CI between *Spiroplasma*-positive males and negative females. The status of *Spiroplasma* infection was initially tested for in the hemolymph of infected females and subsequently in the receiver females of the endosymbiont-free strain STU(-) and their male offspring by PCR with the primers ApDnaAF1 and ApDnaAR1 as described above (also see Table S2) following DNA extraction with the nexttec™ 1^{-Step} DNA Isolation Kit for Tissue & Cells (nexttec Biotechnologie GmbH, Hilgertshausen, Germany) for all samples except the hemolymph. Positive results were confirmed by Sanger Sequencing (Microsynth Seqlab, Göttingen, Germany).

Testing for *Spiroplasma* in the hemolymph

To confirm the presence of *Spiroplasma*, hemolymph was extracted from 20 STU females. The wasps were fixed on a double-sided adhesive tape to a slide and as much hemolymph as possible was removed from the abdomens with a drawn-out glass capillary mounted on a micromanipulator and pooled in 30 µl of TE buffer and 3 µl of proteinase K (nexttec™ 1^{-Step} DNA Isolation Kit for Tissue & Cells; nexttec Biotechnologie GmbH, Hilgertshausen, Germany). This mixture was incubated at 55°C for 30 min and 300 rpm and at 100°C for 10 min for DNA extraction as described by (Holehouse et al., 2003). The presence of *Spiroplasma* was tested for with PCR conditions slightly modified from those specified before by using 40 cycles instead of 35 and by increasing the template volume to 2 µl while decreasing the volume of double distilled water in the PCR mixture by 1 µl accordingly.

Transfer of hemolymph

Donor and receiver females were newly hatched and virgin. Prior to the experiment, receiver females were cooled in a refrigerator at 5°C to reduce their mobility. Hemolymph was extracted from a donor female as described above and subsequently injected with an Eppendorf FemtoJet® (Eppendorf AG, Hamburg, Germany) into the abdomen of a receiver female that was carefully held using a spring steel forceps. The receiver females were transferred to batches of 2 g koi pellets infested with larvae of *S. paniceum* as hosts for oviposition. Host batches were replaced every two to three days until the death of the wasps. After their death, the receiver females were either transferred to 100% ethanol and stored at -20°C until DNA extraction, or immediately extracted. Because they remained unmated, they only produced male offspring. For the subsequent experiments, only male offspring of *Spiroplasma*-positive receiver females were used.

Testing for CI with male offspring

Newly hatched male offspring of positive receiver females were mated to virgin, uninfected STU(-) females. After copulation, the males were killed in 2 ml tubes (Sarstedt AG & Co. KG, Nümbrecht, Germany) containing 100% ethanol and kept at -20°C until DNA extraction unless they were extracted immediately. All samples were subsequently checked for *Spiroplasma* infection. The uninfected STU(-) females were placed on 5 g koi pellets infested with larvae of *S. paniceum* as hosts for oviposition. After four weeks, the number and sex of the F2 offspring were recorded to study CI. Crosses without any offspring were excluded from the analysis.

Effect of *Spiroplasma* titer on CI level

In order to examine whether the strength of CI detected in matings between positive males and tetracycline-treated females was correlated to the *Spiroplasma* load in these males, we conducted quantitative PCR (qPCR) with all samples of mated *Spiroplasma*-positive F1 male offspring of receiver females. *DnaA*, amplified with the primers ApDnaAF1 and ApDnaAR1, was chosen as target gene.

qPCR standards

A PCR product of one of the studied samples was purified using the Thermo Scientific GeneJet Gel extraction and DNA Cleanup Micro Kit (Thermo Fisher Scientific, Waltham MA, USA). The DNA content was checked with an Eppendorf BioPhotometer® D30 (Eppendorf AG, Hamburg, Germany), and the purified

PCR product was cloned into pGEM®-T Easy Vector (Promega, Madison WI, USA), whereby the ligation protocol was modified by using 0.5 µl pGEM®-T Easy Vector (50 ng), 1 µl DNA Ligase (3 U/µl), 2.5 µl 2X Rapid Ligation Buffer, and 2 µl PCR product. The ligation was incubated overnight at 16°C. The ligation mix was then used to transform 45 µl of chemically competent *E. coli* JM109. The transformed bacteria were grown overnight at 37°C and 250 rpm in 20 ml test tubes filled with 5 ml LB-medium containing 100 µg/ml ampicillin. Plasmid extraction was performed using the peqGold Plasmid Miniprep Kit I (VWR International GmbH, Darmstadt, Germany). The plasmid extract was amplified with 2.5 µl DreamTaq™ Green Buffer (Thermo Fisher Scientific, Waltham MA, USA), 2.5 µl dNTPs, 0.125 DreamTaq™ Green DNA Polymerase (Thermo Fisher Scientific, Waltham MA, USA), 18.87 µl double distilled water, and 0.5 µl of each of the sequencing primers SP6/T7 (see Table S2 for details) and sent for Sanger Sequencing (Microsynth Seqlab, Göttingen, Germany) to confirm the *Spiroplasma dnaA* insert. The closest match in the NCBI database was *Spiroplasma* sp. Ozg *dnaA* gene (GenBank: AB586705.1) with 99% identity and 100% query coverage. The concentration of the plasmid extract was measured using a Qubit fluorometer (Thermo Fisher Scientific, Waltham MA, USA), and the original extract was serially diluted (1:10) to serve as standards for qPCR. The standard curve had a slope of -3.501 and a y intercept of 39.256 with a regression coefficient R2 of 0.991. PCR efficiency was determined to be approximately 90%. The range of reliable quantification was determined to be 103 to 1010 target molecules/µl DNA extract, with a Cq variation of 0.25 at the lower boundary.

qPCR

qPCR was conducted on a CFX96 Real Time System (Bio-Rad Laboratories, Inc.) with Platinum® SYBR® Green qPCR SuperMix-UDG (Invitrogen, Carlsbad CA, USA), in reaction volumes of 10 µl, consisting of 0.8 µl template (DNA extract or standard), 5 µl 2x qPCR supermix, 0.2 µl 10mM forward primer, 0.2 µl 10 mM reverse primer, 0.2 µl ROX Reference Dye and 3.6 µl nuclease-free water. The annealing temperature of 52°C was determined by gradient PCR prior to qPCR. A lower elongation temperature of 60°C had to be used to allow amplification of the AT-rich template. The resulting cycling conditions were therefore: 50°C for 2 min; 95°C for 2 min; 35 cycles of 95°C for 20 s, 52°C for 20 s and 60°C for 1 min; followed by recording of the melting curve (50 to 95°C in increments of 0.5°). Two analytic runs were conducted, each with technical duplicates of all samples and standards as well as four non-template controls. The measurements of each sample were averaged for further analyses after excluding outliers according to Grubbs's test (Grubbs, 1950). *Spiroplasma dnaA* copy numbers were calculated by linear regression to the standard curve.

Genome sequencing, assembly, and annotation

Nucleic acids were extracted from a pool of ten adult *L. distinguendus* strain STU using the phenol-chloroform method. Paired-end, 125 bp sequencing libraries were prepared from genomic DNA by Genome Quebec and sequenced on one third of an Illumina HiSeq 2500 lane. The sequencing run yielded 95.5 million reads from which adapters and low-quality sequences were trimmed using bbduk (Bushnell, 2014). A metagenome assembly was assembled using SPAdes 3.10.1 (Bankevich et al., 2012). The *Spiroplasma* metagenome assembly was covered to 30x Illumina read depth (Figure S1), but fragmented. High molecular weight DNA was extracted from a second pool of 25 adult *L. distinguendus* STU adults used to generate 2.1 Gbp of Oxford Nanopore MinION reads on an R9 flow cell. Counting only passed reads over 1000 bases, total sequencing yield was 1.8 Gbp. An initial hybrid metagenome was assembled using Unicycler (Wick et al., 2017). *Spiroplasma*-derived contigs were retained through a combination of metagenomic binning (Laczny et al., 2017) and manual curation. Manual curation involved targeted searches for sequences likely to contaminate the bin based on similar base composition, e.g. host mitochondrial genome, and was guided by kmer abundance analyses performed with KAT (Mapleson et al., 2017). Contigs associated with the lowest and highest 21-mer abundances (Figure S5) were investigated and retained only if BLASTn, BLASTp, or HMMER searches yielded significant similarity with other *Spiroplasma*. In general, the low abundance kmers were unidentifiable or attributable to *L. distinguendus* genome contamination and were removed, while the highest were insertion sequence elements common in Ixodetis clade genomes. Genome completeness was estimated using BUSCO (Simão et al., 2015) implemented on the gVolante webserver (Nishimura et al., 2017). The draft genome was annotated using Prokka 1.14.5 (Seemann, 2014). KEGG numbers were assigned using BLASTKoala (Kanehisa et al., 2016). *Spiroplasma* homologues of interest, including potential toxins (Figure S3, Figure S4, Table S5), plasmid-associated genes (Table S6), and those used for phylogenetics, were identified by tBLASTn, BLASTn, BLASTp and alignments (Altschul et al., 1990). Nucleotide sequences were aligned with MAFFT 7.388

(Katoh and Standley, 2013) and phylograms were built using FastTree 2.1.11 (Price et al., 2010). The GTR substitution model was used to build phylograms from nucleotide alignments and the JTT model was used for amino acid alignments. Protein domains were identified with HMMER 3.3 (Finn et al., 2011) and PfamScan with an expect value threshold of .01 (Madeira et al., 2019). Proteins of interest, including those containing *cif*-like domain homologues were investigated further using HHPRED to identify potentially hidden structural homologies (Zimmermann et al., 2018). BLASTp searches with relaxed significance thresholds (expect values $\leq$ 0.01) were also performed to ensure detection of more distantly related protein domains, if present.

QUANTIFICATION AND STATISTICAL ANALYSIS

Statistical analyses were conducted using RStudio (v. 1.3.1093 (R Core Team, 2020, RStudio Team 2020)) with the packages "multcomp" (Hothorn et al., 2008) and "car" (Fox and Weisberg, 2019) in addition to the pre-installed packages. Statistical significance was assumed at $p < 0.05$, with $p < 0.01$ and $p < 0.001$ indicating high and very high significance, respectively.

To test for CI in crossing experiments between tetracycline-treated and untreated STU individuals, the numbers of male and female F1 offspring as well as total F1 offspring were analyzed with generalized linear models, with negative binomial chosen for family as the best fit, since the data did not adhere to normal distribution. Significant differences and numbers of replicates are indicated in Figure 1; the corresponding *p* values are given in Table S1.

A 2x4 Fisher's Exact Test for Count Data was used to compare the rate of infection with Enterobacteriaceae between tetracycline-treated and untreated STU females as well as CI-inducing and non-CI inducing STU males due to low replicate numbers. Numbers of replicates and *p* values are given in the corresponding section of the results text.

For the comparisons of F2 female offspring numbers as well as F2 male offspring numbers between crosses of STU(-) females with *sDis*-negative and positive F1 male offspring of hemolymph-injected STU(-), Wilcoxon rank sum tests with continuity correction were used due to the data being non-normally distributed. As normal distribution applied to the total F2 offspring numbers of these crosses, they were compared using a Welch two sample t-test. Information on *p, W* and *t* values, levels of significance, and replicates are given in Figure 3B and its legend as well as the corresponding results text.

The correlation between *dnaA* copy number determined by qPCR and the level of CI represented by proportion of female offspring (number of female F2 offspring divided by total number of F2 offspring) was assessed using Spearman's rank correlation, as further detailed in the respective part of the results section.